

Authors' response to all referees for ACP-2019-1181

The authors would like to thank both referees/reviewers for their comprehensive, constructive and insightful comments and for their overall very positive reviews of this work. We have taken care to ensure that we have addressed each comment in detail, and where we have felt it appropriate to do so, we have made changes to the manuscript. As a result of the reviewers' comments and our changes, we feel this paper has been enhanced, making our findings stronger, clearer and easier to follow.

Please find below a breakdown of all referee comments (in black text) with our responses (in **blue text**). Where appropriate, line numbers have been included in our responses, and please note that these refer to the line numbers in the new tracked changes version of the manuscript.

Reviewer 1 (Quentin Libois)

1) A major issue of the paper, which might however be ruled out in a few sentences or with complementary simulations, is the treatment of the atmosphere above the aircraft. Indeed the paper clearly details how the atmosphere is prescribed below the aircraft, but nothing is said about the presence of an atmosphere above the aircraft, suggesting that deep space is considered starting at 9.3 km. At the same time the authors point in the introduction the fact that scattering is important in the FIR (l.46), much larger than in the MIR. This means that any downward flux coming from above the aircraft will be partly reflected in the FIR, hence will contribute to the observed upward radiance. The presence of a cloud above the aircraft or the tiny residual of water vapor at this altitude would certainly be visible. As a consequence the absence of any cloud should be verified and stated as long as possible, and a water vapor profile used for the whole atmosphere (for instance taking a co-located ERA-I profile). A sensitivity study could be performed to ensure that what happens above the aircraft cannot be the reason for the residuals in the FIR. Note that the additional scattering from the cloud would tend to enhance the simulated FIR radiance, which is currently underestimated.

Measurements of the downwelling radiation at the start of SLR 1 from the TAFTS instrument were used to confirm visual impressions from on-board instrument operators at the time of the flight that there were no clouds situated above the aircraft (Figure R1). It should be noted that these TAFTS downwelling observations were used for 'quick-looks' only so have not undergone the full rigorous calibration applied to the upwelling spectra analysed in the paper, which is the reason for some of the negative radiance values in the TAFTS SW channel spectrum.

The observations were compared with simulations of clear-sky downwelling radiance using the nearest ERA-I profile in space and time which, given the spatial and temporal resolution of ERA-I would also be appropriate to use to simulate downwelling radiances for the entirety of SLR1. Figure R1 shows the observations and simulations for the TAFTS SW channel. The simulations and observations show a generally excellent match, particularly in the micro-windows which would be most sensitive to the presence of cloud. In the spectral regions used for the minimisation approach described in the paper (shown by the green triangles), the downwelling radiances from the TAFTS observations are at most $2\text{-}3 \text{ mW m}^{-2} \text{ sr}^{-1} (\text{cm}^{-1})^{-1}$ (within instrument noise for this first calibration effort), while the simulated spectrum indicates lower values of almost zero. These low values, combined with the predominantly forward scattering characteristics of the ice particles, show that outside of strong water vapour lines (not used in the minimisation) there is negligible contribution to the observed upwelling radiation as a result of reflected downwelling radiation from above the aircraft.

We have added a sentence at **lines 126-127** to confirm that establishing that there was no evidence of the presence of a cloud above the aircraft at the time of the nadir radiance observations for the cases considered was also a requirement.

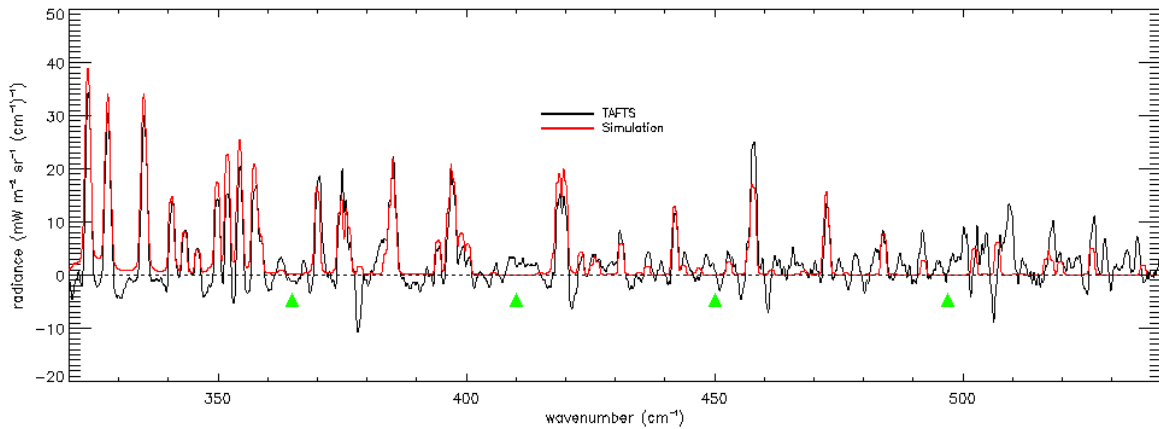


Figure R1: Downwelling radiance spectra at the aircraft as observed by TAFTS (black) at the start of SLR1 and simulated (red) using ERA-I profiles for T and WV (assuming a standard mid latitude winter profile for all other atmospheric components), for the SW channel.

2) The objective of the paper is to demonstrate that current SSPs databases don't work throughout the MIR and FIR spectral ranges. However to demonstrate this only one database is used, that of Baum et al. (2014). Why weren't more extensive databases used, in particular those of Yang et al. (2013) including a larger variety of habits and the effect of roughness, which is mentioned in the introduction (l.30) but not further. Also, could the database of Baran et al. (2014) be used as well? Consider also that of van Diedenhoven and Cairns (2020) to be exhaustive. If none of those databases (which probably cover all the available databases) manage to reconcile the MIR and the FIR, then the conclusion of the paper would be much stronger. At least, it should be specified to which extent the presently used database is representative of all those available in the literature.

We have amended the text to be more explicit that the databases tested and the approach used is not the only means by which cirrus radiative effects can be simulated (**lines 89-91**). However, we would point out that Baum's database does in fact include roughness and explicitly uses several of the habits modelled by Yang et al. (2013) to build the aggregate SSPs we test here, informed by extensive field campaign measurements. We agree that Baran's database would be interesting to test but it is currently being revised (Baran, personal communication, 2019) so would prefer to wait until the newer version is ready. The Van Diedenhoven and Cairns (2020) approach is a parameterisation specifically for climate models which is evaluated in part by comparison to Yang et al. (2013) and in part via comparison to the ice model used in the MODIS C6 ice cloud retrieval products (severely roughened aggregates of columns). Apart from the difficulty in including this parameterisation when the paper describing it was published after this manuscript was submitted, it seems counter-productive to use an approach which itself is evaluated via comparison to the models that already contribute to those tested here.

3) The authors mention an exhaustive set of optical probes, many of them providing detailed information about the ice crystals habits and size distributions. Although it is clear that taking these information as a raw input to the simulations wouldn't work, at least because of the elapsed time between the radiative and microphysical observations, these rich observations are not mentioned at all. Maybe the complexity of the habits, the singularity of the PSDs would point to possible deficiencies

of the SSPs databases. Also this could provide useful information regarding the vertical structure of the clouds, which is currently too quickly ruled out as a potential explanation for the inadequacy observed and would deserve more investigation and a dedicated sensitivity study.

We have addressed this as part of a more detailed response to a related question from Reviewer 2. Please see our response to Reviewer 2, General Comment 2.

4) More generally, the paper would greatly benefit from physical insight about the limitations of the databases. In which direction should experts work ? What's the next step ? Could you inform whether the temperature dependence of the refractive index may solve something. To do so it should depend on the spectral range, does it ? What about surface roughness etc. ? Such discussion could of course be very exploratory but would have the merit to provide meaningful leads for improvement.

We are observationalists at heart so in our opinion the critical next step is actually to generate a more complete observational database than the one case study analysed here. In particular we need a suite of comprehensive observations that encompasses the entire EM spectrum, with good cross-calibration where appropriate, and simultaneously measure the cloud microphysics, over a range of different cirrus cloud regimes (not simply frontal cloud as analysed here). This is explicitly stated in the paper. We do think that investigating the temperature dependence of the refractive index of ice has merit since studies have shown that the single scattering property response is more pronounced across the far infrared (greatest impact on scattering between 30 to 50 μm and absorption from 20 to 40 μm) compared to the mid infrared [Iwabuchi and Yang., 2011] with implications for ice cloud retrievals [Saito et al., 2020]. Currently, to the best of our knowledge, suitable databases incorporating this sensitivity for application to spectrally resolved measurements do not exist.

Whilst the Baum database we use already includes surface roughness, Maestri et al. (2019) noted that for thin cirrus their simulated downwelling spectra showed little sensitivity to surface roughness from smooth to severely roughened. This would suggest that this is not the major deficiency, although further observational data and associated studies would help confirm to what extent this is important.

Text has been added and amended between **lines 364-370** to reflect questions over the limitations of the current optical databases and references added accordingly.

References:

Maestri, T., C. Arosio, R. Rizzi, L. Palchetti, G. Bianchini and M. Del Guasta: Antarctic ice cloud identification and properties using downwelling spectral radiance from 100 to 1,400 cm^{-1} , *J. Geophys. Res. Atmos.*, 124, 4761-4781, doi:10.1029/2018JD029205, 2019.

Saito, M., Yang, P., Huang, X., Brindley, H. E., Mlynczak, M. G. and Kahn, B. H.: Spaceborne mid- and far-infrared observations improving nighttime ice cloud property retrievals. *Geophys. Res. Lett.*, *in press*, 2020.

5) What are the practical consequences of the paper for energy budgets or for ice cloud retrievals? How is cirrus radiative effect erroneous in climate simulations, how does it matter? How comes that radiative closures have been satisfying in the MIR if adding FIR channels would have resulted in different parameters? Do FIR channels provide significantly different retrievals, or do they narrow the range of possible values (hence uncertainties)?

We consider the first three questions here to be too big to address comprehensively in this paper. We have given a rough estimate of the longwave flux impact for this specific case but it would not be appropriate to speculate what this might be on a global scale given all the factors that influence the cloud radiative effect (as discussed in the paper's introduction). We show here that the radiative

effects are less than 1 W m^{-2} when integrated from $110\text{--}1400 \text{ cm}^{-1}$, which is substantially better than the instantaneous accuracy of current broadband flux observations and hence might well be considered a satisfactory match. The main point we make is that adding the far infrared information highlights how this match is comprised of compensating effects which would not be revealed by a broadband comparison. So, given current space-based observational tools (which do not measure the spectrum across the FIR) we may not actually know how ‘wrong’ climate model simulations are – only new observations and comparisons can reveal this.

We also caveat again that we cannot match across the MIR and FIR simultaneously, to with the observational uncertainties, using the models tested here so our flux estimate is in some senses not representative of what the ‘real’ discrepancy might be, even for this single case.

6) Here is a suggestion to illustrate the differences in FIR and MIR retrievals for one selected case. On a 2D LUT with re_{eff} and τ as axes (assuming a fixed habit), highlight the regions corresponding to MIR and FIR matching (for the different methods). This would help understand the minimisation procedure and indicate in which direction FIR channels tend to drive the retrievals (for instance).

There are no simulations that simultaneously match across both regimes; this has now been emphasized (line 317). So it is not possible to see in which direction the FIR retrievals drive the MIR ones as the two sub-sets are independent of one another.

Technical corrections

I.15 : single-scattering is probably more detailed than “optical” so should not be in parentheses

Single-scattering has been removed to be consistent with the terminology used in the title.

I.18 : state whether those fluxes are broadband or spectral

This has been clarified by adding “spectral” (line 19)

I.19 : “strong” is not quantitative, is it ± 2 or $\pm 10 \text{ W m}^{-2}$? Not clear how there can be a compensation between something that is within the residuals and something that is not.

“strong” has been removed. Here we are making the general point that the best performing set of optical properties (in terms of generating minimum radiance residuals) result in a compensation effect between the FIR and MIR. The implication of this is that this compensation may not be apparent if simulations are simply evaluated against broadband flux measurements, which is typical for climate models.

I.22 : “cloud properties” is not defined, and the link to retrieval is not that straightforward.

This sentence has been removed.

I.23 : “guidance” is probably not sufficient currently for the practical development of new databases

This sentence has been removed.

I.26 : an additional sentence to present the SW (thin so often limited albedo) and LW (cold so large greenhouse effect) effects of cirrus clouds may be useful before talking about net effect.

A sentence has been added to clarify the contrasting impact of clouds on incoming solar and emitted thermal radiation in the context of published results (line 32).

I.27 : “geographical position” is not very clear. How does it impact the radiative effect? Do you mean temperature contrast with the local surface and atmosphere ? This last point should not overlap with the first two characteristics pointed out. Also, given the subsequent definition of the microphysical properties, I feel like optical thickness or particle number concentration is lacking here, unless it is included in the PSD (at its zeroth moment)

“Geographical location” simply means latitude/longitude since, as the reviewer notes, this determines surface type. Sentence has been split in two to make the dependencies clearer, and optical thickness has been specifically mentioned (line 36).

I.35 : I tend to write *in situ* as it is a Latin phrase. Holds elsewhere

The formatting guidelines for the ACP Journal indicate that these should not be italicised. Therefore we have made no change.

I.38 : do the authors mean that all ice clouds are cirrus clouds or that they focus on cirri only ? Ice clouds could be tackled more broadly.

Clearly we are focusing on cirri here. However, some of the literature is more generic, and includes all ice cloud. We have revised the wording slightly in lines 31-36 to help clarify, and then focused specifically on cirrus.

I.42 : no lower wavenumber limit given for the FIR ? Can be misleading

Actually, to the best of our knowledge there is no universally accepted lower (or even upper) bound for the FIR. It varies across communities and even within the atmospheric physics community itself. But, to be broadly consistent with the measurements we analyse here we have chosen 100-600 cm⁻¹. The text at line 53 has been amended accordingly.

I.45 : the formulation “sensitivie to radiation” is unclear. Do you mean that the optical properties are highly variable across the FIR ? That the broadband properties are sensitive to what happens in the FIR ?

The text has been amended to indicate that FIR radiation is highly sensitive to the optical properties (line 56).

I.49 : maybe state that this holds for narrowband channels, not necessarily for hyperspectral observations

We have added “narrowband” for clarity (line 60).

I.51 : “spectrally-resolved” has not been properly defined. Maybe give a hint to which spectral resolution this refers, because depending whether the reader is a climate modeler or a spectroscopist the expectations might differ.

There are no global observations specifically covering the FIR whether these are hyperspectral or narrowband (or even integrated from 100-600 cm⁻¹) – therefore we think that defining a specific resolution here is not really helpful. We have amended the sentence to reflect this paucity (lines 63-64).

I.94 : could you detail if relevant what those probes measure : PSD, scattering properties, habit ? Are all these instruments used in the paper? Are they to some extent redundant? Only relevant data should be presented.

We have added this information in **line 110**. Although the data are not used directly here for the reasons explained in the paper, it is an obvious question to ask whether such data were available and so it makes sense to provide a brief summary. We have removed the detailed information on size ranges as this is not necessary.

I.96 : how are cloud phase and total amount of ice measured ?

Discussion of the cloud phase and issues with determining the phase of particles smaller than 50 μm for example, along with estimates of the ice water content derived from the different probes are covered in O'Shea *et al.*, (2016). However, to the best of our knowledge, total ice water content was not estimated from the probes. The lidar was used to estimate the ice volume extinction profiles as stated.

I.98 : "information" is vague, do you mean geometric thickness here, as extinction follows ?

Yes, this has been clarified by changing "profile" to "extent" (**line 114**).

I.100 : here more details on the assumptions to convert backscatter profiles into extinction profiles are needed because (as discussed later on) this is key for the consistency of the synergistic radiative closure.

In response to Reviewer 2, comment "p.8 I.257", we have now amended the discussion of the discrepancy between the lidar optical depth and that inferred from simulations of the observed radiances (see **lines 286-292**). We also now note (**lines 290-292**) that the required adjustment of the optical depth does not undermine the use of the relative variation of the extinction with height or the cloud thickness. Given this and considering that we do not use the optical depth from the lidar (except as a first guess) we feel that additional detail on the lidar processing is not needed here. We think that the reference provided [Fox *et al.*, 2019] (now **line 116**) is sufficient since they provide details of the processing and a full discussion of the lidar data used here.

I.108: knowledge of the atmospheric profile above the aircraft is key as well because of scattering (including backscattering from the clouds). In particular, the absence of clouds above the aircraft is critical.

The impact of downwelling radiation from above the aircraft reflected by the cloud has been demonstrated to be negligible (see response to Reviewer 1, comment 1). We have added a sentence at **lines 126-127** to state that an additional requirement is that no cloud should be present above the aircraft.

I.117: the acquisition time of a TAFTS spectrum is lacking to understand why and how 3 sets of radiance can be taken in 1 min 12 s. Please also clarify the ARIES acquisition time.

We do not feel that the operational cycles of the interferometers are relevant to this paper since we are using the observations that are available to us given the clearly stated selection criteria. However, more details on TAFTS and ARIES can be found in Bellisario *et al.* [2017] and also Magurno *et al.* [2020].

References:

Bellisario, C. and co-authors: Retrievals of the Far Infrared Surface Emissivity Over the Greenland Plateau Using the Tropospheric Airborne Fourier Transform Spectrometer (TAFTS), *JGR Atmos.*, doi:10.1002/2017JD027328, 2017.

Magurno, D. and co-authors: Cirrus cloud identification from airborne far-infrared and mid-infrared spectra, *Remote Sens.* 2020, 12(13), 2097; doi:10.3390/rs12132097, 2020.

I.120: what does this “two second period” refer to? It is not clear

This is the +/- 1 s of the TAFTS acquisition time referred to in the previous sentence.

I.121: what’s the reason for converting radiance spectra into brightness temperature (BT)? Is it practical when it comes to including instrumental error, which is more uniform in radiance than in BT?

We think it is easier to show differences in brightness temperature and relate to physical properties than using the radiances. Also, yes, the uncertainties quoted for ARIES were only available expressed as a brightness temperature estimate.

I.125: what “variations in the cirrus properties” do you refer to? Do you simply mean the presence of cirrus ?

This refers to the variation between cases A, B and C which at this point we do not speculate whether this is cloud top temperature, cloud optical depth or cloud microphysical properties. Therefore, no this isn’t the presence of cirrus, we are just pointing out that the cloud has different radiative properties between cases A, B and C. Therefore, we hope the existing text is appropriate and sufficient.

I.127: why is that “useful”? Is this used further in the study? Is it original, unexpected, instructive?

Useful was perhaps a bad choice of word and this has been changed to ‘interesting’ (line 144). This simply points out that the relative variation across the spectral regions, particularly where the impact of the cloud on the observed radiation is visible (i.e. in the window regions in the MIR and micro-window regions in the FIR), is not consistent for all three cases. This, we hope, suggests that the impact of the cloud on the radiation in these micro-windows is varied and complex (as we go on to discuss later in the paragraph).

I.131: “a frequency dependent sensitivity to cirrus properties” is unclear. Sensitivity of what?

A frequency dependent sensitivity of cloud’s radiative signature to the cirrus properties. The text has been amended to clarify this (lines 148, 149).

I.145: are these really two radiative codes, or does LBLDIS merge the LBLRTM model for gas optical thickness and DISORT for the radiative transfer equation solver?

Yes these are two distinct codes, LBLRTM calculates the spectrally resolved transmission of the atmospheric layers given temperature profiles and concentrations of chosen atmospheric absorbers. This is a standalone routine that does not require LBLDIS. However, LBLRTM cannot calculate the impact of scattering from ice crystals. Therefore LBLDIS, which is essentially a routine for running the radiative transfer code, DISORT, is required to calculate the impact of the scattering and absorption of the cloud properties, combined with the spectrally resolved transmission. It does require the output from LBLRTM as you correctly point out. However, we feel that these are two distinct routines for which references have been provided.

I.148: this should be more explicit that most parameterizations try to express the single scattering properties in terms of the effective radius. Note also that it differs from the approach of Baran et al. (2014) who use temperature and ice water content to estimate single scattering properties.

We do not understand this comment. The text clearly states the simulation methodology, which follows an approach that is commonly used. Whilst we appreciate that Baran has an alternative way of relating the optical properties of an ice cloud, we are only using the optical depth and effective radius of a size distribution.

I.152: this match is surprisingly low

This is the level of agreement we see between the datasets. Perhaps the reviewer would like to elaborate why this is worthy of further comment in the paper. ‘Low’ is quite hard to interpret.

I.153: does this emissivity model spectrally extend into the FIR?

No, the longest wavelength is 13 μm ($\sim 769 \text{ cm}^{-1}$). A sentence has been added to clarify that the Masuda model only applies for wavenumbers down to $\sim 769 \text{ cm}^{-1}$ (line 170), and a spectrally invariant value of 0.99 was used for lower frequencies (lines 171-172). However, the opaque nature of the atmosphere in the FIR between the surface and cirrus cloud means that there is no impact of the FIR surface emissivity on the aircraft measured radiances (lines 172-173).

I.154: again, no information about what the atmosphere above the aircraft looks like, although this may be critical

Please see our response to your comment “1”).

I.169: how many streams were used?

16 – this information has been added in line 190.

I.171: why only focusing on these 3 databases while Yang et al. (2013) proposes much more? In particular the effect of roughness could be investigated as a solution to overcome the current deficiencies.

Please see our response to your comment “2”)

I.197: separated into → composed of, split into, discretised into ?

“separated into” has been changed to “split into” (line 220).

I.218: The Baum model was already mentioned

Indeed, but this refers to the particular Baum model – the Aggregate Solid Columns (ASC).

I.227: how wide are these spectral regions?

A single channel is $\sim 2 \text{ cm}^{-1}$ in each spectral region to avoid a dilution in the sensitivity of the minimisation to strong absorption features not attributed to the cloud properties (e.g. water vapour). The channel width is now clarified (line 256).

I.231: is this “ τ ” referring to a single cloud layer, or to the whole cloud? Is the profile still scaled on the lidar profile? Also precise whether habit and r_{eff} are assumed vertically homogeneous.

Optical depth refers to the entire cloud, the profile was scaled using the lidar profile and r_{eff} was assumed vertically homogeneous. An extra sentence has been added to the figure caption for “Table 2” to indicate this and there is also substantial extra discussion in section 4.2 to address a comment from Reviewer 2.

I.241: could you explain what is the physical meaning of weighting by the error? What differences do you expect in comparison with the second approach? Why duplicating similar approaches?

Weighting the differences by the uncertainty allows the relative importance of the difference compared to the uncertainty in each minimisation region to be taken into account. This is similar to a Chi Square approach. Following a comment from Reviewer 2 “p.8 I.235”, the minimisation method of

Eq. 1 was repeated using a Chi Square. The same results were obtained for the Chi Square approach as when using Eq.1. The second approach simply looks at the total error assuming that all uncertainties are equal across the spectrum.

Since the approach used to determine the differences does not fundamentally impact the conclusion, that no single simulated spectrum can match the observations across the entire mid and far-infrared, we feel it is helpful to retain both approaches.

I.242: are the Rs in the formula spectra? In which case how is the absolute difference defined? Unless one wavenumber region is actually a single channel? This should be clarified

One wavenumber region is a single channel ($\sim 2 \text{ cm}^{-1}$ wide). This is clarified by the new wording in **lines 255-256** which now does not use 'region'.

I.244: is the minimisation performed through interpolation (or selection) of the LUT, or using a dedicated algorithm?

Selection. The discretisation of the parameters (e.g. optical depth, effective radius of the particle size distribution) was chosen to be sufficient that the observational uncertainties were much greater than the quantised variability of the simulated radiative spectra.

I.257: can such an inconsistency really explain 45% differences?

It is our understanding that the primary source of the uncertainty remains in the selection of the lidar ratio to produce a volume extinction coefficient. However, since the lidar extinction profiles are simply used to constrain the vertical extent of the cloud and provide an estimate of the relative IWC profile within the cloud, we do not seek to account for these differences. We feel this is beyond the scope of this paper. However, please also see response to Reviewer 2, "p.8 I.257" and updates in **lines 286-292**.

I.258: Details are needed to clarify the lidar estimate of extinction

Please see response to Reviewer 2, "p.8 I.257".

I.260: why using two methods which are so close, in particular if the consistency is not surprising (I.274)?

This indicates that the variation in the estimated uncertainties in the observed spectral radiances is not a key influence on the result. However, we feel it is useful to present both methods. Also see response to your comment "I.241".

I.282: do these 14 simulations refer to method 4? Otherwise it reads like they are those among the 739 that also match FIR observations, which is obviously not the case reading the following sentence. More explicitly, matching has not been properly defined. It is generally completed by "within uncertainties", which is clear for MIR, but not for FIR. Maybe the difference between match in the selected channels and across the whole spectrum should also be more clearly explained.

Yes. Additional words have been added to clarify this point (**line 317**). This was actually stated in the sentence following the original I282 but this has now been removed as it would simply repeat the information contained in the revised **line 317**.

I.289-290: this suggests that no combination works in the FIR? So I guess the 14 spectra mentioned previously were matching only for the selected channels.

Yes, this is hopefully clear following the amendment to answer the previous comment (**line 317**).

I.291: this is not clear why retrieval would be more constrained. If no set of parameters works, then what to conclude? Something that is sure is that using different spectral regions for the retrieval gives different results, which is of course worth pointing. But speaking of retrieval quality sounds hazardous so far.

We agree, this could be misinterpreted. We have replaced the sentence with one that more accurately captures our intent – to state that the combination of FIR and MIR measurements can provide a more rigorous test of the ability of ice cloud optical property models to correctly capture the cloud radiative signature than MIR observations alone (lines 326-327).

I.295: could there be a spectral signature of the angular signal? Maybe look at spectra at 3 different viewing angles to ensure that this approximation is acceptable.

This figure is provided as rough estimate only as stated in the text. A more thorough treatment would be required to definitively answer this point, possibly using more than 3 viewing angles. In addition, simulations at angles other than nadir would also make the assumption that the angular scattering of the cirrus is correctly (or at least consistently well) captured by the optical models across the spectral range sampled, which might be unlikely given the results shown here.

I.297: if this compensation occurs within the uncertainty range of observations, can it be considered significant? Physically, does it mean that among the possible parameters after MIR matching, FIR selects the largest/smallest r_{eff} or optical thickness? This compensation should be further discussed because this provides physical insight about what individual spectral ranges would try to converge to (specific comment 6).

We reiterate: there is no combination of r_{eff} and optical depth that allows us to simultaneously match across the MIR and FIR within the uncertainties. Please also see our response to your comment 6.

I.301: there is no more mention of the minimisation methods. Which method results in 2 W m⁻² errors?

Hopefully this is clear that now that Table 4 includes results from all four approaches used (in response to a comment from Reviewer 2). The text also indicates that method 3 (and now method 4) provides discrepancies that exceed 2 W m⁻² in lines 339-340.

I.301: I think that at this stage the main conclusion should be that none of the optical models investigated allows to match observations, which points to the need for new models. It is a result and should be mentioned before the next paragraph.

We do not understand the need to repeat this message here.

I.305: state-of-the-art for sure, but encompassing all those available in the literature?

We do not use all available in the literature, please see response to your comment "2)" for further details. However the statement clearly refers to the Baum optical models, which themselves have been shown to represent the optical properties of ice clouds in the MIR based on an extensive series of field campaigns.

I.308: "tested here" suggests that other models could work, so makes the conclusions weaker

As you note in your comment "2)" we have not tested all models so therefore feel this wording is appropriate.

I.313: how can you be sure that this tighter constraint result in a better retrieval? I think a retrieval quality should be regarded through the uncertainty associated with this retrieval, not only through the absolute error of the optimal parameters. In that sense, how does adding FIR observations help reducing the retrieval possibilities is informative.

This is an interesting question, but we feel it is one that is beyond the scope of this paper. We do not actually say anything about retrievals here.

I.314: the habit was not much discussed for the retrieval. If it is forced, are the optimal reff and optical depths significantly different?

We would like to reemphasize that we are not performing a retrieval. We are looking for the simulation that most closely matches the observations. However, to answer your question, we re-ran the minimisation using approach 1, forcing the habit to be confined to the ASC for Case A. The closest matching spectrum related to a simulation using an increased optical depth of ~ 0.06 (compared with unconstrained habit presented in the results), and the effective radius of the PSD increased from 34 to $40 \mu\text{m}$. The corresponding absolute flux differences for the three bands (MIR, SW FIR and LW FIR – i.e. the 3 columns from table 4) using approach 1 were: 1.11 (1.10), 1.18 (-0.64), 0.25 (-0.08) W m^{-2} . Therefore fixing the habit does of course affect the choice of simulated spectrum most closely matching the observation, but this increases the differences (as would be expected), and hence is worse. We hope this answers your question, but we do not think this is relevant information to include in the paper.

I.315: energy analysis is most meaningful at global scale. Could you provide hints to the expected global error given the distribution of cirrus (occurrence and optical depth). If 2 W m^{-2} is specific to the case studied here, it could have limited implications in a climate framework.

Not necessarily for all applications but we agree the general point from a climate perspective. However, it is impossible to give a hint on what the global error would be from this single case study given all the factors that influence cirrus radiative effect as discussed in the introduction, not least the optical thickness.

I.320: Could you, based on your simulations, provide a more quantitative (adding a figure for instance) discussion of this potential impact on the heating rates? This would bring the attention of the climate modelers. Maybe comparing the heating/cooling rates profiles of the 4 methods for the same case.

We think this is beyond the scope of this paper. We hope that the pointer we provide in the discussion might motivate further study into the potential effects on vertical heating rates. This same comment also applies to your previous point (“I.315”).

I.324. If temperature dependence is a potential venue, could you briefly explain why this may help reconcile MIR and FIR. For this, some different sensitivities should exist in this temperature dependence between the FIR and MIR. Is that the case? The personal communication could be expanded.

We now point towards the paper by Iwabuchi and Yang [2011] which demonstrates the impact of this temperature dependence spectrally, and to some new work by Saito et al. [2020] (lines 364 to 368).

I.326: this is indeed an important point, but not sufficiently detailed. How was this vertical heterogeneity investigated? What vertical gradients were used? How could cloud probes provide quantitative information about this vertical layering? So far, the short explanation lacks details to rule out the possibility that vertical layering associated with distinct penetration depth into the cloud of

the MIR and FIR (because of scattering) could be a reason for the observed mismatch. Especially when looking at the sensitivity displayed in Figure 6a.

[Please see our response to Reviewer 2, General Comment 1.](#)

I.331: does this mean that “new” parameterizations were built as in Baum et al. (2014) based on these new PSDs? Alike the other leads investigated, this should be quantified more properly, in terms of error bars associated with this kind of assumption of the PSDs. Other theoretical PSDs (different shapes, different widths) could also be investigated.

[Yes, using Ping Yang’s individual optical models \(Baum’s are a hybrid of these\), new PSDs were generated. However, for reasons already mentioned, the observations are poorly constrained given the time difference and variability of the cloud reported by the lidar and indeed the variability seen within the in-situ data itself. For this reason we do not see the value of providing a detailed description of these studies. Please also see our response to Reviewer 2, General Comment 2.](#)

I.339: how do you solve the issue of concomitant cloud microphysics observation in the spaceborne configuration? Accounting for the mismatch of spatial scales.

[Whilst this is an important question, we do not think this is something that this paper should be asked to address. In order to answer this, it would require an entirely new study in its own right, however, we can say that dedicated under-flights with suitable instrumentation will obviously be required.](#)

I.340: how long is the journey to the ultimate information? Again for the modelers, the paper would benefit from providing concrete leads towards improvement. Said differently, how should a climate modeler take these results?

[The goal of this paper is to make researchers, including climate modellers, understand that there remain significant uncertainties in representing the optical properties of ice clouds consistently across the infrared and that these uncertainties can propagate to sizeable radiative effects that might not be manifested in broadband comparisons. We think the paper conveys this message.](#)

Table 3: the retrieved habit for the method 3 differs from all the others. Would there be an explanation why including FIR observations tends to constrain the habit to GHM?

[The most likely explanation is the enhanced sensitivity to habit in the far-infrared \(see Fig. 6b\) compared to a relatively flat response in the mid-infrared.](#)

Table 4: none of the broadband fluxes differences reaches 2 W m⁻², which seems contradictory with the statement in the text (I.301).

[Broadband refers to the 3 “broadband channels” of LW FIR \(110 to 300 cm⁻¹\), SW FIR \(320 to 540 cm⁻¹\) and MIR \(600 to 1400 cm⁻¹\). Therefore Table 4 shows that for approach #3 for case B, there is a negative difference of -2.02. However, as a result of a request by Reviewer 2 to include all 4 approaches, there are now many more examples of this value reaching and exceeding 2 Wm⁻².](#)

Reviewer 2 (Anonymous Referee #1)

General comments:

1. My first thought about the discrepancy of retrieved optical properties in the two spectral ranges was, that the observations might be sensitive to different depths of the cloud. In the discussion, it is

mentioned, that this has been investigated by varying the r_{eff} -profile within the cloud layer and it was found, that the profile has only a minor impact. I suggest to include this investigation, at least as a short appendix, rather than just mention it in one sentence in the discussion, because this is also an important result.

This has now been added in **Section 4.2**. Your comment motivated a re-examination of the sensitivity which has improved Figure 6 such that the baseline simulation is now consistent across all four perturbation experiments (this was not previously the case). Because of this the results show larger sensitivity to a perturbation in the vertical profile of r_{eff} than was originally reported but this would not be distinguishable from a vertically uniform perturbation in r_{eff} and has a much smaller magnitude (compare Fig. 6(a) to 6(d)). For this reason we continue to assume r_{eff} is vertically uniform in our approach since incorporating vertical variation would not change our overall conclusion regarding the FIR-MIR inconsistency.

The text has been updated in Section 4.2 to account for the addition of Fig. 6(d), and also the other changes made. A new Fig.6 has been produced and the figure caption updated accordingly.

2. The in-situ observations are mentioned in the "Instrumentation and measurements" section but are not used because "examination of the available in-situ cloud microphysical properties [O'Shea et al., 2016] also indicated a high temporal (and therefore implied spatial) variation in the cloud PSD. These issues, combined with the knowledge that the cloud was decaying over time, suggested that it would be difficult to associate a particular observed PSD with any confidence to the radiation measurements." (p.7 l.194) - I agree that it is often difficult to compare with the in-situ observations. However, I think that you should try to at least compare the results with the in-situ observations. E.g., is the habit distribution observed in-situ similar to the general habit mixture as used by Baum et al. or is it dominated by aggregates of solid columns?

The derived PSD from in-situ should also be included for comparison, even though it may not be possible to directly compare it to the results derived from the radiance observations.

We think it is important to point out that we are not trying to hide anything by not including the in-situ results, simply that the rapid evolution of the cloud system being studied coupled with the 50 minute (to over two hours) delay between the radiative observations and the in-situ observations makes the comparison pointless since we really aren't sampling the same cloud. Indeed, as we now mention in the text (**Section 4.1**) the in-situ measurements themselves show a rapid variation over the period that they were collected. However, for information, we include below the relevant plots from O'Shea et al. [2016]. These are derived from the in-situ observations, binned according to cloud temperature (a proxy for altitude). These indicate that there was no consistently dominant habit, with perhaps the exception of the coldest layer sampled within the cloud, during the in-situ measurements (Figure 6 (b)).

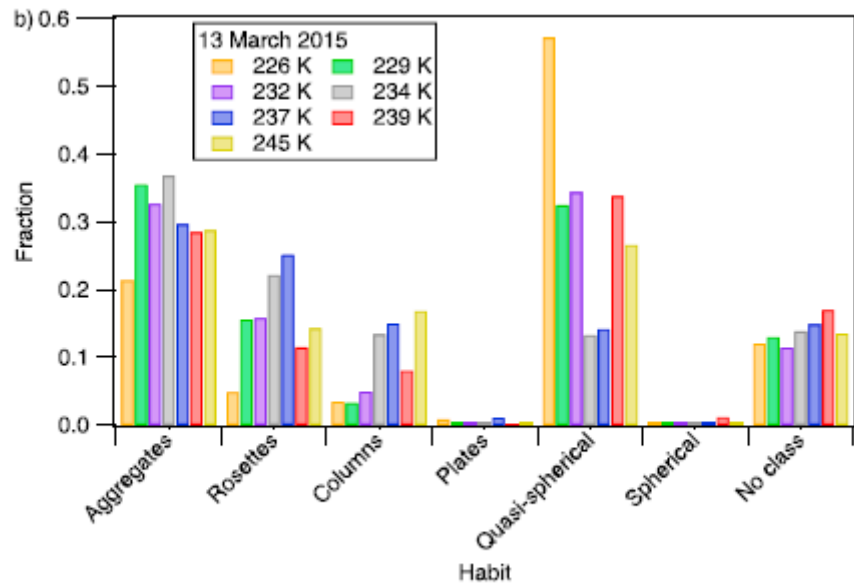


Figure 6. Proportions of particle habits observed by the CPI within different temperature regions of the clouds for (a) 11 March 2015 and (b) 13 March 2015. The temperatures correspond to the same runs/profiles shown in Figure 5.

They also suggest a variable PSD which may have a temperature-size dependence (Figure 5(b)) but this was difficult to quantify given the uncertainties surrounding the measurements of the smaller ice particles made by the 2DS (O’Shea, Pers. Comm. 2019), further questioning the value of examining the PSD data for this study. However, very recent work, soon to be submitted for publication may improve the understanding of the 2DS data and its comparison with the HALOHolo (O’Shea, Pers. Comm. 2020).

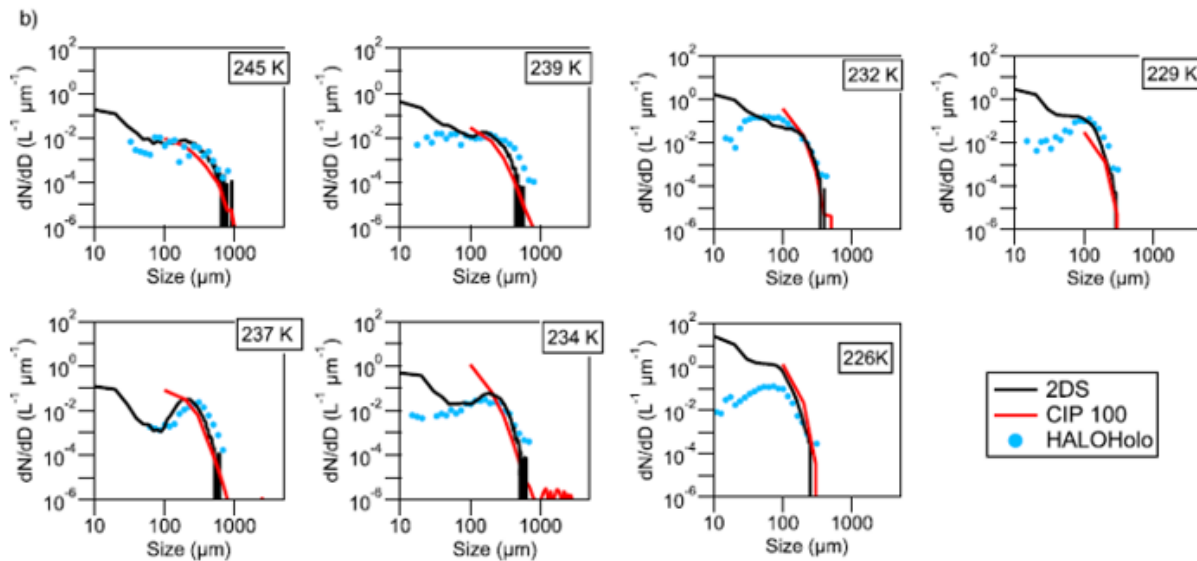


Figure 5. (continued)

O’Shea et al. [2016] Figure 5 (adapted). Particle size distributions from the 2DS (black lines) and CIP 100 (red lines) probes for different temperature regions for (b) 13 March 2015. HALOHolo observations are shown in blue. The PSDs have been averaged over individual runs/profiles made by the FAAM BAe-146.

Figures 5(b) and 6 (b) shown above have been reproduced from O’Shea et al. [2016] with permission from the author. The original figures are available online

<https://agupubs.onlinelibrary.wiley.com/doi/full/10.1002/2016JD025278> (open access).

Specific comments

p.5 l.159: Where are the "present day concentrations" of CO₂ and minor trace gases obtained from?

These were obtained from the NOAA-ESRL measurements from Mace Head, a reference has been added at **lines 179-180**.

p.7 l.206: "a similar overestimate seem relative to the TAFTS measurements in the FIR micro-windows." -> I can not see this in Fig. 5, a difference plot could help.

Closer examination of the differences in fact show that the differences in the MIR are around 4 K and only around 2 K in FIR. The text at **line 229** has been amended to indicate this. We have included a difference plot here (Fig. R2) for completeness but do not feel it adds much to the paper, since the differences between the observations and simulations are examined in much greater detail in Fig. 7.

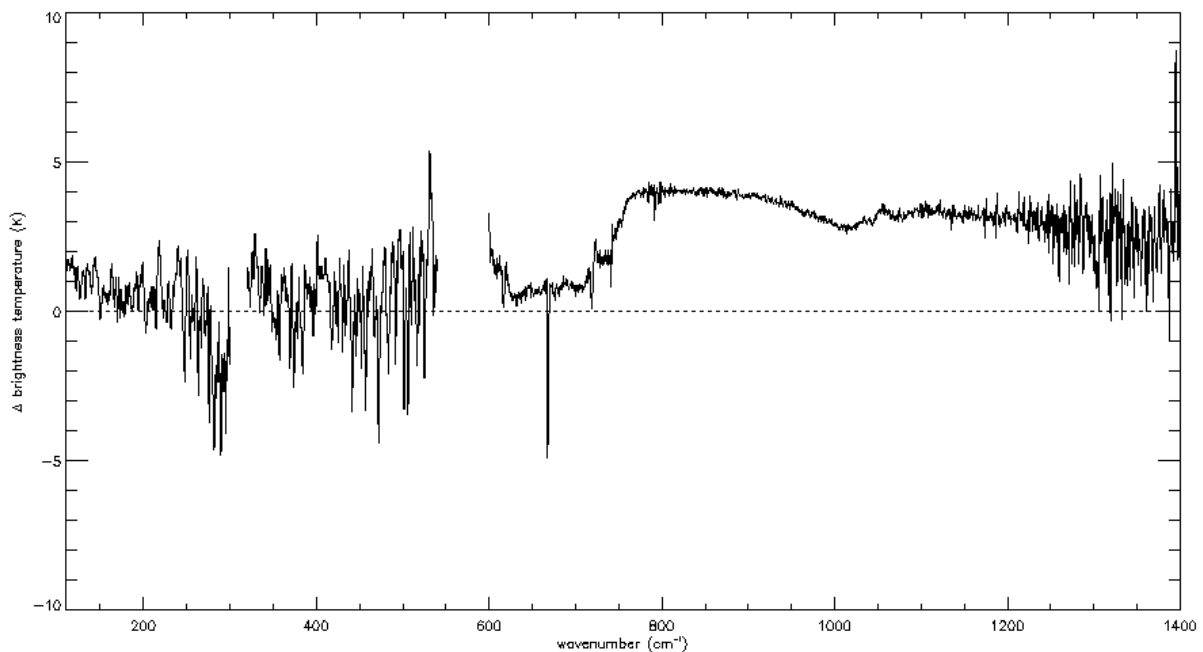


Figure R2: Simulation minus observation relating to the observed and simulated (cloudy-sky) spectra shown in Fig. 5.

p.8 l.235: Eq. 1 and 2: Why are absolute differences used in the fit, rather than the more commonly used quadratic differences (Chi-square fit)?

Equation 1 weights the differences by the uncertainty, allowing the relative importance of the difference compared to the uncertainty in each minimisation region to be taken into account. This is similar to a Chi Square approach. To check, this was repeated using a Chi Square, and the same results were obtained to those using Eq.1.

The second approach (Eq. 2) simply looks at the total error implicitly assuming that all uncertainties are equal across the spectrum. This was included as an alternative way to identify the best matching simulations to the observations. Irrespective of the approach used, there is no impact on the conclusion, that no single simulated spectrum can match the observations across the entire mid and far-infrared.

p.8 l.257: The lidar-derived value of optical thickness is smaller than that retrieved from the fit. "The deviation may be a consequence of an inconsistency between the optical properties implicitly assumed when converting the raw lidar measurements to optical depth compared with those used in the simulations here". This is a plausible explanation. Which optical properties are assumed in the lidar observation?

We have rephrased the discussion of the lidar optical depth (lines 286-292) to better reflect the way the lidar data are processed, since the lidar optical depth is derived from the lidar extinction which is a function of the lidar extinction-to-backscatter ratio, commonly referred to as the lidar ratio. This ratio is a function of the optical properties of the cloud but is determined directly from the lidar dataset rather than being derived via a cloud microphysical model. A more detailed explanation follows.

In this study we used the Baum models to enable wavelength interpolation of the lidar optical depth determined at 355 nm. The lidar optical depth was determined from the lidar derived volume extinction coefficient at 355 nm and the lidar observed cloud thickness. The lidar data were analysed to obtain profiles of both the extinction coefficient and backscatter. This was carried out using a constant value of the backscatter to extinction ratio (lidar ratio) of 25 sr [Fox et al., 2019] which is considered typical for cirrus [e.g. Young et al., 2013]. However, the value of this ratio is expected to vary with the details of the cloud microphysics, and both theoretical [e.g. Ding et al., 2016] and observational [e.g. Chen et al., 2002; Gouveia et al., 2017] studies indicate that variations of roughly +/- 50% around of this value are not unusual.

Therefore, adjustment of the lidar ratio well within this plausible range would produce a lidar optical depth consistent with the values obtained from the simulations (i.e the closest matching simulation to the observations). Although strictly speaking applying such an adjustment within the lidar processing would induce subtly different corrections within the profile, over the extinction coefficient range here this effect is expected to be negligible compared to other sources of measurement error. Hence in this analysis, we simply use the lidar data as processed, to provide information on the cloud geometrical thickness and the relative variation of extinction within the cloud (and for a "first guess" of the cloud optical depth). We then scale the derived optical depth, noting that the scaling required to provide agreement between the lidar and the simulations is not outside of what might be expected.

We have clarified in the text that the scaling of the lidar optical depth is analogous to adjusting the assumed backscatter-to-extinction (lidar) ratio from the mean value used. We note that this is within the plausible range for cirrus, and this would not significantly impact the lidar determined relative variation of the extinction within the cloud or its geometrical extent.

References:

Chen, W-N., Chiang, C-W. and Nee, J-B.: Lidar ratio and depolarization ratio for cirrus clouds, *Appl. Opt.*, 41, 6470-6476, doi: 10.1364/AO.41.006470, 2002.

Ding, J., Yang, P., Holz, R. E., Platnick, S., Meyer, K. G., Vaughan, M. A., Hu, Y. and King, M. D.: Ice cloud backscatter study and comparison with CALIPSO and MODIS satellite data, *Opt. Expr.*, 620, doi.org/10.1364/OE.24.000620, 2016.

Fox, S., Mendrok, J., Eriksson, P., Ekelund, R., O'Shea, S. J., Bower, K. N., Baran, A. J., Harlow, R. C. and Pickering, J. C.: Airborne validation of radiative transfer modelling of ice clouds at millimetre and sub-millimetre wavelengths, *Atmos. Meas. Tech.*, 12, 1599-1617, doi:10.5194/amt-12-1599-2019, 2019.

Gouveia, D. A., Barja, B., Barbosa, H. M. J., Seifert, P., Baars, H., Pauliquevis, T. Artaxo, P.: Optical and geometrical properties of cirrus clouds in Amazonia derived from 1 year of ground-based lidar measurements, *Atmos. Chem. Phys.*, 17, 3619–3636, doi:10.5194/acp-17-3619-2017, 2017.

Young, S. A., Vaughan, M. A., Kuehn, R. E., and Winker, D. M.: The Retrieval of Profiles of Particulate Extinction from Cloud-Aerosol Lidar and Infrared Pathfinder Satellite Observations (CALIPSO) Data: Uncertainty and Error Sensitivity Analyses, *J. Atmos. Ocean. Tech.*, 30, 395–428, doi:10.1175/JTECH-D-12-00046.1, 2013.

Fig. 7: For consistency, the transmittance should also be included in the upper panel. The transmittance curve should have a different color than "Method 1", it is particular confusing, because "Method 1" is often overplotted and not visible.

[The transmittance has been added to the upper panel and the colour has been changed.](#)

Table 4: Results from "Method 4" should be added, even though future observations restricted only to FIR are not anticipated.

[These results have now been added.](#)

A test of the ability of current bulk optical models to represent the radiative properties of cirrus cloud across the mid- and far-infrared

Richard J. Bantges^{1,2}, Helen E. Brindley^{1,2}, Jonathan E. Murray², Alan E. Last², Jacqueline E. Russell²,
Cathryn Fox³, Stuart Fox³, Chawn Harlow³, Sebastian J. O'Shea⁴, Keith N. Bower⁴, Bryan A. Baum⁵,
Ping Yang⁶, Hilke Oetjen⁷ and Juliet C. Pickering²

¹National Centre for Earth Observation, Imperial College London, UK

²Physics Department, Imperial College London, UK

³Met Office, UK

⁴University of Manchester, UK

⁵Science and Technology Corporation, Madison, USA

⁶Department of Atmospheric Sciences, Texas A&M University, USA

⁷ESA/ESTEC, Noordwijk, Netherlands

Correspondence to: Richard J. Bantges (r.bantges@imperial.ac.uk)

Abstract. Measurements of mid- to far-infrared nadir radiances obtained from the UK Facility for Airborne Atmospheric Measurements (FAAM) BAe-146 aircraft during the Cirrus Coupled Cloud-Radiation Experiment (CIRCCREX) are used to assess the performance of various ice cloud bulk optical (~~single scattering~~) property models. Through use of a minimisation approach, we find that the simulations can reproduce the observed spectra in the mid-infrared to within measurement uncertainty but are unable to simultaneously match the observations over the far-infrared frequency range. When both mid and far-infrared observations are used to minimise residuals, first order estimates of the spectral flux differences between the best performing simulations and observations indicate a ~~strong~~ compensation effect between the mid- and far-infrared such that the absolute broadband difference is $< 0.7 \text{ W m}^{-2}$. However, simply matching the spectra using the mid-infrared (far-infrared) observations in isolation leads to substantially larger discrepancies, with absolute differences reaching ~ 1.8 (3.1) W m^{-2} . These results show that simulations using these microphysical models may give a broadly correct integrated longwave radiative impact but that this masks spectral errors, with implicit consequences for the vertical distribution of atmospheric heating. They also imply that retrievals using these models applied to mid-infrared radiances in isolation will select cirrus optical properties that are inconsistent with far-infrared radiances. As such they highlight the potential benefit of more extensive far-infrared observations for the assessment and, where necessary, the improvement of current ice bulk highlight the benefit of far infrared observations for better constraining retrievals of cirrus cloud properties and their radiative impact, and provide guidance for the development of more realistic ice cloud optical models.

1 Introduction

The role of ice clouds (e.g. cirrus) in determining the radiative balance of the Earth and its atmosphere is particularly complex and uncertain [e.g. Baran et al., 2014b; Yang et al., 2015]. Recent calculations based on ice cloud properties retrieved from

active satellite instruments suggest that ice clouds have a net warming effect on the global climate, with enhanced trapping of outgoing infrared radiation, particularly from cirrus anvils, exceeding enhanced reflection of incoming solar radiation [Hong et al., 2016]. More generally, the net radiative effect of all types of ice cloud, including cirrus, is critically dependent upon its optical thickness, which itself is linked to the cloud microphysical properties. Other important characteristics include The net radiative effect of cirrus is dependent upon its microphysical properties, the vertical position and extent, and the geographical location of the cloud [e.g. Heymsfield et al., 2013; Hong and Liu, 2015]. Key microphysical parameters include ice particle habit, particle size distribution (PSD), and morphology such as aggregation, roughness and concavity [Zhang et al., 1999; Baran, 2012; Yang et al., 2012; Baum et al., 2014]. However, these parameters vary both temporally and spatially, and are dependent on the changes in temperature, humidity, and meteorological environment that the cloud experiences [Yang et al., 2012; Baran et al., 2015; Voigt et al., 2017].

To accurately predict the radiative effect of cirrus in Global Climate and Numerical Weather Prediction models the interaction of radiation with the ice particles that make up the cloud must be known. This relationship is reliant on knowledge of cirrus optical properties which are currently poorly constrained [Baran, 2012]. Nevertheless, several cirrus bulk optical (single-scattering) property models have been developed using in situ observations and databases of ice single scattering properties (SSPs), which aim to include realistic physical representations of ice particles, including habit, aggregation and roughness [Yang et al., 2008, 2012; Baran et al., 2014a,b; Baum et al., 2014].

A key test for these cirrus models is whether, when constrained by suitable in situ observations, they are able to replicate simultaneous radiance observations across the electromagnetic spectrum. Previous assessments of model consistency with observations in the solar and mid-infrared (MIR: typically defined as wavenumbers from \sim 600 to 2500 cm^{-1}) [e.g. Baran and Francis, 2004; Baum et al., 2014; Platnick et al., 2017; Loeb et al., 2018; Yang et al., 2018] have shown reasonable agreement, however there have been very few studies performed in the far-infrared (FIR: defined here as wavenumbers from \sim 100 to $<$ 600 cm^{-1}). It is particularly important to validate cirrus models in the FIR as, not only does this region contribute of the order 50 % of the outgoing longwave radiation in the global mean [Harries et al., 2008], but theoretical studies have also indicated that the radiation is highly sensitive to the ice particle optical properties are highly sensitive to radiation in this region [e.g. Maestri and Rizzi, 2003; Baran, 2005, 2007]. In particular, Edwards and Slingo [1996] and Kuo et al. [2017] show that scattering by cirrus clouds in the far-infrared regime contributes substantially to longwave radiation observed at the top of the atmosphere (TOA). The effect of neglecting longwave scattering is comparable to the effect associated with doubling CO₂. Moreover, it has been demonstrated that the addition of a few narrowband FIR channels to the MIR channels typically used in satellite retrieval algorithms could significantly improve our ability to retrieve ice cloud radiative properties [Libois and Blanchet, 2017].

However, compared to the well-studied MIR, spectrally resolved global observations specifically measuring across the FIR are unavailable. There are some narrowband and spectrally resolved measurements available, however, from focused field campaigns. Maestri et al. [2014] analysed downwelling FIR spectral radiances in the presence of cirrus as recorded by the REFIR-PAD instrument [Bianchini and Palchetti, 2008] at the ground-based Testa Grigia station (Italy), 3500 m above sea

level, during the Earth COoling by WAter vapouR emission (ECOWAR) campaign. Retrieved cloud properties from the MIR were used to simulate radiances in the region $250\text{--}1100\text{ cm}^{-1}$. Unsurprisingly these showed excellent agreement with the observations in the MIR window from $820\text{--}960\text{ cm}^{-1}$ but large residuals were apparent in the FIR from $330\text{--}600\text{ cm}^{-1}$. More recent work by Palchetti et al. [2016] and di Natale et al. [2017] suggests that simulated and observed downwelling radiances at the surface can be reconciled within uncertainties across much of the FIR and MIR range if temperature, water vapour and cirrus properties are simultaneously retrieved from the observations. [Maestri et al. \[2019\] reported the first tentative retrievals of ice particle habit from downwelling FIR spectra obtained by REFIR-PAD over Antarctica in 2013, although they noted that large residuals in their retrievals did not permit clear identification of ice particle habit in most cases.](#)

Maestri et al. [2014] also discussed the advantages of a ‘view-from-above’ (satellite or aircraft) experimental configuration for the study of FIR cirrus optical properties. A further benefit of aircraft campaigns for performing model validation exercises is that in principle the radiative signature of the clouds can be recorded closely in time with in situ measurements of the cloud microphysics, allowing them to be linked directly [Baran and Francis, 2004; Maestri, 2005]. However, to the best of our knowledge, the only published study based on simultaneous aircraft observations of MIR and FIR radiances in the presence of cirrus is that of Cox et al. [2010]. This study concluded that simulations were not able to consistently reproduce observed spectral radiances across the infrared and were particularly poor in the FIR region $330\text{--}600\text{ cm}^{-1}$, where the analysis was hampered by the presence of large uncertainties in the atmospheric state and a lack of instrumentation capable of measuring small ice particles (diameter $< 20\text{ }\mu\text{m}$).

Here we make use of upwelling radiances recorded above cirrus across both the FIR and MIR spectral regions simultaneously during the Cirrus Coupled Cloud-Radiation Experiment (CIRCCREX), a flight campaign using the Facility for Airborne Atmospheric Measurements (FAAM) British Aerospace (BAe) 146 aircraft based out of Prestwick, Scotland. We focus on flight B895 which took place over the North Sea to the north east of Scotland on the 13th March 2015 and test, for the first time, the ability of the bulk optical models for cirrus developed by Yang et al. [2013] and Baum et al. [2014] to reproduce radiance observations across the infrared including the FIR. [Although these by no means represent the only resource for simulating cirrus radiative effects \(e.g. Baran et al. \[2014b\]; van Diedenhoven and Cairns \[2020\]\) they are widely used by the remote sensing community and so warrant investigation.](#) The paper is organised as follows: section 2 provides a summary of the flight and the measurements obtained, along with details of how suitable case studies were identified. Section 3 describes the methodology applied to simulate the observed FIR and MIR spectra and the performance criteria for assessing the “best” matches between observations and simulations. The results are presented in section 4 with conclusions from the study drawn in section 5.

2. Observational data

2.1 Flight B895 overview

The FAAM flight B895 left Prestwick in the UK on the 13th March 2015, and overflew a decaying band of cirrus cloud associated with an occluded front. The main objective of the flight was to characterise both the cirrus cloud microphysics and 100 their associated IR radiative signatures. To achieve this aim, the aircraft performed a series of straight and level runs (SLRs) above the cloud followed by a descent into the cloud deck where a further series of SLRs were performed at varying levels within the cloud. Figures 1(a) and (b) show the flight track and altitude of the aircraft as a function of time, respectively.

2.2 Instrumentation and measurements

The FAAM aircraft was fitted with a ‘cloud-radiation’ suite of instruments which included radiation sensors, cloud 105 microphysical probes and a lidar. The radiation instruments included two Fourier transform spectrometers: the Tropospheric Airborne Fourier Transform Spectrometer (TAFTS, Canas et al. 1997) with nominal spectral coverage from 80 cm^{-1} to 600 cm^{-1} (two channels: LW from 80 cm^{-1} to 300 cm^{-1} , and SW from 320 cm^{-1} to 600 cm^{-1}) operating at 0.12 cm^{-1} resolution, and the Airborne Research Interferometer Evaluation System (ARIES, Wilson et al. 1999) with nominal spectral coverage from 550 cm^{-1} to 3000 cm^{-1} (two channels: LW from 550 cm^{-1} to 1800 cm^{-1} and SW from 1700 cm^{-1} to 3000 cm^{-1}) at 1 cm^{-1} resolution. The cloud microphysics (PSD and habit) were measured using a series of probes that included a 2DS, a 3 View- 110 Cloud Particle Imager (3V-CPI), CIP 100 and a holographic cloud probe (HALO Holo), [Lawson et al., 2006; O’Shea et al., 2016]. ~~The 2DS and 3V-CPI are capable of sampling particle sizes from 10 to 1280 μm , the CIP 100 from 100 to 6400 μm and the HALO Holo from 6 μm to 1 cm.~~ The lidar installed on the aircraft was a Leosphere ALS450 355nm elastic backscatter lidar [Marenco, 2010] which provided cloud vertical profile extent information and ice volume extinction profiles at 355 nm from 115 the range-corrected backscatter profiles following the two-stage process of Marenco et al. [2011]. Vertical profiles of particle extinction coefficient were estimated [Fox et al., 2019] from which the cloud optical depth at 355 nm, (τ_{355}), was derived. Finally, along with the standard aircraft positioning sensors, temperature and humidity sensors, the aircraft was also equipped with the Airborne Vertical Atmospheric Profiling System (AVAPS) [Vaisala, 1999] which launched RD94 dropsondes [Vaisala, 2010] at various stages in the flight to enable characterisation of the atmospheric column below the aircraft.

120 2.3 Identification of suitable case studies

The driving factor in selecting periods for analysis was the availability of near-simultaneous TAFTS and ARIES nadir radiance spectra from SLRs above the cloud. Ideally, simulation of radiance spectra equivalent to those observed at the aircraft level above the cirrus cloud requires knowledge of the cloud microphysical and optical properties, its vertical location and the atmospheric profile from the surface to the aircraft. Hence, additional selection criteria were that cirrus could be clearly 125 identified and characterised by the lidar observations and that the atmospheric state below the aircraft was well-characterised

by dropsonde measurements. The final requirement was that the atmosphere above the aircraft was cloud-free to ensure that any downwelling radiation from above the aircraft, reflected by the cloud beneath, could be ignored.

Preliminary examination of the available data from the three above-cloud SLRs suggested that there were two periods which satisfied these requirements; one during SLR 1 from 09:48:39 to 09:49:51 UTC and another during SLR 3 from 10:16:22 to 10:17:24 UTC. Unfortunately, ARIES data from the period identified in SLR 3 were found to have deficiencies [S Fox, pers. comm. 2019], and considered to have insufficient quality for the purpose of this study. Consequently, only those data from the period during SLR 1 were considered for further investigation. Three sets of radiance observations were identified from within SLR 1: the times of these observations along with a summary of the conditions at the aircraft are summarised in Table 1.

For each of the three cases identified, only a single TAFTS spectrum was available; however, owing to the relatively high temporal sampling frequency of the ARIES instrument, eight ARIES spectra are available within ± 1 s of the TAFTS acquisition time. To provide an indication of the scene variability within the two second period around the TAFTS measurement, the mean and associated standard deviation are calculated for the eight ARIES radiance spectra. The mean ARIES and the associated TAFTS spectra are then converted into equivalent brightness temperature spectra. These are shown for all three cases in Fig. 2. In the MIR, signatures of cirrus are most apparent in the main atmospheric window (~ 760 - 1000 , 1080 - 1250 cm^{-1}) as indicated in Fig. 2 (c). At FIR frequencies, the atmosphere is less transparent because water vapour absorption fills in many spectral lines, but there are a series of semi-transparent, so called “micro-windows” as shown in Fig. 2 (b), that clearly show the variation in the cirrus properties. For the lowest frequencies in the FIR, the atmosphere is comparatively opaque with generally a much lower sensitivity (less than 1 K) to the cirrus with the exception of a few wavenumber regions (e.g. ~ 110 cm^{-1} , 218 to 221 cm^{-1} , 240 cm^{-1} , etc.). It is useful interesting to note that there is a variation in the ordering of the three cases between the different spectral regions. For example, at around 110 cm^{-1} the maximum brightness temperature is observed for case C followed by B and then A; case B shows the highest values in micro-window 3 (around 410 cm^{-1}) followed by A and then C; in the MIR window regions the largest values are for case A, followed by B and then C. The variation in the relative ordering of the individual cases indicates a frequency dependent sensitivity of the cloud’s radiative signature to the cirrus properties: this sensitivity to the ice particle size and habit is discussed further in section 4.2.

Figure 3(a) shows the lidar extinction profiles for the three cases (A-C). Panels (b) and (c) show the atmospheric temperature and water vapour mixing ratio profiles obtained from the two dropsondes deployed nearest to the time of the selected radiance observations at 09:47:48 UTC (ds1) and 09:50:52 (ds2). The aircraft altitude is shown by the dashed red line. The extinction profiles derived from the lidar measurements indicate a band of cirrus was located between approximately 6 and 9 km in altitude with no evidence of any underlying cloud. Integration of these extinction profiles for the three cases, from 6 to 9 km, indicates that τ_{355} ranged from approximately 0.53 to 0.59. These clouds would therefore typically have been classified as optically thin [e.g. Dessler and Yang, 2003]. Examination of ds1 and ds2 demonstrates that between their deployments the atmospheric state remained relatively stable, with a noticeably dry layer between approximately 3 and 5 km evident in both water vapour profiles. There is a degree of variability in the temperature profile around 4 km, and in the water vapour mixing ratio below 3 km. The impact of this variability on the simulated radiance spectra is discussed in section 4.

3. Simulation methodology

The simulation approach makes use of two radiative transfer models, the Line by Line Radiative Transfer Model (LBLRTM, [Clough et al., 2005]) and the Line by Line Discrete Ordinates (LBLDIS v3.0, [Turner, 2005]) code, in conjunction with a representation of the atmospheric state including cloud location and microphysics, expressed in terms of optical depth and effective radius.

For all three cases simulated the aircraft was overflying ocean. The radiative temperature of the ocean surface was assumed to equal the temperature measured at the lowest altitude from the closest dropsonde in time to the radiance observation. These values were compared to collocated European Centre for Medium Range Weather Forecasts (ECMWF) Interim Reanalysis (ERA-I; [Dee et al., 2011]) surface skin temperatures and were found in all cases to agree to within 0.1 K. The ocean surface

170 spectral emissivity was defined, for wavenumbers down to $\sim 769 \text{ cm}^{-1}$, using the wind-speed dependent model from Masuda et al. [1988], with estimates of the wind speed obtained from the nearest available ERA-I value. The ocean surface spectral emissivity for wavenumbers lower than $\sim 769 \text{ cm}^{-1}$ was set to 0.99 although the impact of this choice is negligible given the strong water vapour absorption between the surface and cloud level in the FIR.

The atmospheric column beneath the aircraft was divided into 0.1 km thick layers, providing 93 layers from the surface to 9.3 km, with an additional layer closest to the aircraft varying in thickness depending upon the aircraft altitude (between 0.085 and 0.091 km). Temperature and water vapour concentrations for each layer were obtained by interpolating the corresponding dropsonde measurements onto the 0.1 km vertical grid, with the exception of the layer closest to the aircraft which was prescribed by the onboard measurements. In the absence of direct measurements, concentrations of carbon dioxide and minor trace gases were obtained from a standard Mid-

175 Latitude Winter (MLW) atmospheric profile [Anderson et al., 1986] and scaled to present day concentrations using data from Mace Head [Dlugokencky et al., 2019]. Ozone concentrations were obtained from collocated ERA-I data and interpolated to the required vertical resolution.

The quantities describing the surface and atmospheric column were then input into LBLRTM to calculate the optical depths for every layer in the atmosphere between the surface and the aircraft over the spectral range 105 cm^{-1} to 1600 cm^{-1} . The latest version currently available, LBLRTM v12.8, was used with the molecular absorption defined by the Atmospheric and 185 Environmental Research (AER) v3.6 spectral line database which is based on the HITRAN 2012 database [Rothman et al., 2013]. The water vapour continuum was defined by the recently released MlawerTobin_Clough-Kneizys-Davies (MT_CKD) 3.2 [Mlawer et al., 2019].

The wavelength-dependent LBLRTM-derived layer optical depths were then passed to LBLDIS, which takes into account scattering by particles in the cloud layer via the Discrete Ordinate Radiative Transfer (DISORT) code [Stamnes et al., 2000].

190 In this study the bulk optical properties used to simulate cloudy radiances were those provided by Baum et al. [2014] using 16 streams. This parameterisation consists of three databases that are based on different ice particle habits: solid columns only

(SC); the aggregate of solid columns only (ASC); and a general habit mixture (GHM) that incorporates plates, droxtals, hollow and solid columns, hollow and solid bullet rosettes, an aggregate of solid columns and a small/large aggregate of plates. Further details on the geometries of these habits are given in Baum et al. [2011] while the method by which the parameterisation was built is reported in Baum et al. [2005a, 2005b, 2007]. Each database contains the SSPs expressed as a function of wavelength (0.2 to 100 μm) for a range of PSDs, assuming a gamma distribution (see Heymsfield et al. [2013]), with particle effective radius (r_{eff}) ranging from 5 to 60 μm . LBLDIS also requires the cloud height, r_{eff} , and optical depth for each cloud layer as input. Based on these input parameters, LBLDIS is used to simulate radiances over a wavenumber range and with a spectral resolution set by the user.

Appropriate instrument apodisation functions were then applied to the simulated radiance spectra. To ensure that this process did not introduce errors, the simulations were performed at 0.01 cm^{-1} resolution. Once the instrument apodisation functions had been applied, the simulated spectra were interpolated onto the same wavenumber scale as the observations, facilitating direct comparison. A schematic summarising the simulation methodology is provided in Fig. 4.

4. Results

We separate the results into three sub-sections. The first section describes the initial efforts to simulate the observed spectra utilising the best available information on the cirrus cloud properties. The following section describes the minimisation methods adopted to find the best agreement between the simulated and observed spectra and the results using these methods are presented in the final section.

4.1 Initial simulation

A single aircraft is not able to simultaneously measure in situ cloud properties and above cloud radiance spectra. Here, the in situ cloud microphysical measurements were obtained over a period of one hour and 20 minutes, starting from approximately 50 minutes after the radiation observations were obtained (Fig. 1). While the cloud vertical structure remained relatively constant during Cases A-C (Fig. 3a), the lidar observations indicated significant variability in the geometrical thickness of the observed cloud during the three SLRs as a whole. Moreover, previous Examination examination of the available in situ cloud microphysical properties [O'Shea et al., 2016] also indicated a high degree of variability in the PSDs and a wide variety of ice particle habits, which were summarised for seven different temperatures (altitudes) sampled within the cloud (see figures 5b and 6b in O'Shea et al. [2016]) ~~temporal (and therefore implied spatial) variation in the cloud PSD~~. These issues, combined with the knowledge that the cloud was decaying over time, suggested that it would be difficult impossible to associate a particular observed PSD or habit with any confidence to the radiation measurements. Therefore, we chose to perform an initial simulation for each case ~~was performed~~ for a cloud, separated split into layers 0.1 km thick, of vertical extent from 6 to 9 km and taking bulk optical properties from the Baum et al. [2014] ASC ice particle habit model, and assuming a fixed $r_{\text{eff}} = 30 \mu\text{m}$

for all layers within the cloud. The relative optical depth for each cloud layer was derived from the lidar observations, ensuring the cloud's total optical depth was equal to the appropriate value from Table 1.

Figure 5 shows the results of such a simulation for case A. For reference, the equivalent clear-sky simulation is also shown.

225 The estimated uncertainty associated with the ARIES spectral calibration is approximately 1 K [S Fox, Met. Office, Personal Communication, 2019], while the 1σ variability in the eight ARIES spectra matched to the TAFTS acquisition time is approximately ± 0.5 K. We therefore estimate the total uncertainty on a mean ARIES spectrum as these values added in quadrature, so ~ 1.1 K. However, the simulated brightness temperature spectrum overestimates the observed ARIES values in the main atmospheric window by around 5.4 K, with a similar smaller (~ 2 K) overestimate also seen relative to the TAFTS 230 measurements in the FIR micro-windows. Conversely, the level of agreement in the strong CO₂ absorption band from 650 to 700 cm⁻¹ (excluding the spike in the centre of the band at 667 cm⁻¹), indicates that the temperature of the uppermost layer in the simulation (i.e. close to the aircraft) is well represented in the temperature profile used in the simulation. These differences point to issues with the cloud properties used in the initial simulation, especially given that interchanging dropsondes 1 and 2 has a comparatively small impact on the simulated spectrum.

235 4.2 Achieving an improved simulation-observation fit

It is evident from Fig. 5 that the initial choice of cloud parameters used to simulate the observed radiance were sub-optimal. The two key parameters typically required to define the microphysical properties of an ice cloud are r_{eff} and the ice particle habit. The sensitivity of the mid-infrared to ice particle size has been known for many years [e.g. Bantges et al., 1999] and more recently sensitivity studies extending into the far-infrared have been performed [e.g. Yang, 2003; Yang et al., 2013].

240 Figure 6 (a-c) shows the results of a series of simulations performed to examine the impact of varying r_{eff} , ice particle habit and optical depth for case A.; the simulated radiances are developed using the Baum et al. [2014] models. As part of this analysis, while we have no direct observational evidence for a variation in r_{eff} with height through the cloud it is reasonable to explore the response to such a variation since it might be expected to be different in the MIR and FIR regimes. Hence Figure 6(d) shows the impact of varying r_{eff} in three 1 km thick layers through the cloud.

245 The results Figure 6 (a) indicate that there are a wide range of spectral regions that demonstrate sensitivity to size from approximately 300 to 500-600 cm⁻¹, 750 to 850 cm⁻¹ and 950 to 1250 cm⁻¹. Note however that the ordering of the differences changes around 400 cm⁻¹ where the largest r_{eff} no longer shows the greatest sensitivity. In contrast, there are spectral regions that exhibit sensitivity primarily to ice particle habit (Fig. 6(b)). Differences between the ASC-GHM and SC model are greatest around 550-500 cm⁻¹, while they are greatest at around 400 cm⁻¹ for ASC-GHM and GHM-ASC differences. Sensitivity to 250 increasing optical depth (Fig. 6(c)) is broadly similar across the MIR and FIR from 400 to 1400 cm⁻¹, but drops off rapidly at wavenumbers lower than 400 cm⁻¹ due to the increasing effect of strong water vapour absorption and the overall reduction in radiative energy at these frequencies. Introducing a vertical variation in r_{eff} (Fig. 6(d)) produces a change which has a very similar spectral shape, but much smaller magnitude, to that observed for a bulk change in r_{eff} .

255 ~~With use of Using~~ this information, a scheme was developed to minimise the differences between the simulated and observed spectra in regions showing particular sensitivity to r_{eff} and habit. Four wavenumber ~~regions channels~~ in the MIR and four in the FIR were used; 775, 850, 900 and 1200 cm^{-1} in the MIR and 365, 410, 450 and 497 cm^{-1} in the FIR, each of $\sim 2 \text{ cm}^{-1}$ width. The ultimate goal was to investigate whether there was any combination of parameters that could fit the observations across the MIR and FIR simultaneously given measurement uncertainties. Because of the reduced sensitivity to the vertical profile of r_{eff} and the similarity of the associated spectral signature to those generated from vertically uniform perturbations to r_{eff} we do not attempt to account for any vertical variation in our simulations.

260

To facilitate the minimisation a series of simulations were performed for a range of r_{eff} and τ for the three ice particle habits in the Baum et al. [2014] database. Table 2 provides a summary of the ranges covered for each variable. These values were chosen, based on initial simulation attempts to match the observed spectrum, to produce a range of simulations that encompassed the observations and their associated uncertainties.

265 The simulations were compiled into a database ordered by τ_{355} , r_{eff} and ice particle habit. Four different approaches were then adopted to identify the simulation that most closely matched the observations for each case. The first approach comprised two stages. The initial stage identified those simulated radiance spectra that agreed to within the measurement uncertainties for the ARIES spectrum for all four of the selected MIR channels to create a subset of ‘matched’ simulated spectra. This subset was then processed to find the simulation that most closely matched the corresponding TAFTS SW spectrum for the four channels 270 identified in the FIR. The absolute difference between the simulations and observations for each FIR channel was weighted by the observation uncertainty and then summed,

$$x = \sum_{i=1}^4 \frac{|R_{\text{sim}i} - R_{\text{obs}i}|}{R_{\text{error}i}} \quad [1]$$

where $R_{\text{sim}i}$ and $R_{\text{obs}i}$ are the simulated and observed radiances, respectively and $R_{\text{error}i}$ is the observation uncertainty for FIR channel i . X was then minimised to obtain the ‘best’ solution.

275 The second approach also comprised two stages, with the first stage mimicking that of the first approach. In the second step the uncertainty weighting was removed such that the minimum of equation 2 was sought,

$$x' = \sum_{i=1}^4 |R_{\text{sim}i} - R_{\text{obs}i}| \quad [2].$$

The third approach focussed on determining the best agreement that could be obtained using the individual MIR spectral range. This was achieved by minimising the integrated absolute difference between the simulation and observation across the MIR 280 from 600 to 1400 cm^{-1} . For completeness, a fourth approach, similar to the third, but in this case minimising the integrated difference in the FIR from 320 to 540 cm^{-1} , was considered to demonstrate whether agreement solely in the FIR could be achieved.

4.3 Minimisation results

The combinations of ice particle habit, r_{eff} and τ_{355} giving the simulated spectra that most closely match the observations using 285 each of the three minimisation methods are summarised in Table 3. The results for all the methods indicate a need to increase

$\tau_{355\text{nm}}$ above the lidar-derived value by ~~between 25 to 45 %, somewhat more than would be anticipated given the estimated an amount larger than the stated~~ uncertainty in the lidar values ~~are of~~ $\pm 20\%$ [S. Fox, pers. comm., 2019]. ~~However, The required change to the derived optical depth can be produced by adjusting the lidar backscatter-to-cloud extinction ratio from the flight-averaged value used in this study [Fox et al., 2019] to values that still lie within the typical range observed for ice clouds [e.g. Chen et al., 2002; Heymsfield et al., 2008; Young et al., 2013; Gouveia et al., 2017]. We note that changing this value would not significantly impact the lidar determined relative variation of the extinction or the cloud geometrical thickness used in this study. deviation may be a consequence of an inconsistency between the optical properties implicitly assumed when converting the raw lidar measurements to optical depth compared with those used in the simulations here [e.g. Heymsfield et al., 2008; Fox et al., 2019].~~

290 Minimisation methods 1 and 2 yield very similar results, both indicating that the GHM habit provides the closest agreement, with the only difference that method 1 suggests a slightly smaller r_{eff} compared to method 2 for Case A. Method 3 demonstrates that using the MIR in isolation gives markedly different values. In this case the results would suggest a cloud comprised of relatively small ASC habit ice particles with an optical depth slightly larger than that indicated by methods 1 and 2. Finally, when matching the FIR observations in isolation (method 4), a cloud with lower optical depth composed of relatively large 295 GHM habit ice particles is implied.

300 The spectral differences between the observations and best matching simulations are shown in Fig. 7 for each minimisation method, separated into 3 different spectral regions defined as MIR (600 to 1400 cm^{-1}), SW FIR (320 to 540 cm^{-1}) and LW FIR (110 to 300 cm^{-1}). It is important to note that the large differences consistently found around 667 cm^{-1} are most likely a measurement artefact due to the extremely strong absorption by CO_2 around this frequency. This results in measurements reflecting the temperature of the air inside or very close to the ARIES instrument. Similar effects can be present due to strong water vapour lines and are particularly evident at wavenumbers $> 1300\text{ cm}^{-1}$. As evidenced by Fig. 3, cloud signatures are more apparent in the more transparent spectral regions indicated by the “window” labels in Fig. 7(a) and where the atmospheric transmission between the cloud-top and aircraft is close to 1 (Figs. 7(b) and (c)).

305 Unsurprisingly given the values in Table 2, the difference spectra from methods 1 and 2 lie almost on top of each other across the full spectral range analysed. Within the MIR (Fig. 7(a)), the differences are within the measurement uncertainties with the exception of those spectral regions most strongly influenced by CO_2 and water vapour discussed above. Within the TAFTS LW channel (Fig. 7(c)), the simulations overlie each other since, as shown in Fig. 6, for frequencies lower than around 300 cm^{-1} , the models predict a greatly reduced sensitivity to ice particle habit and size. The atmospheric layer above the cloud, in this spectral region is also less transparent, further reducing the observed impact of variations in the ice particle properties.

310 315 However, in the SW FIR there are several regions (e.g. 375 cm^{-1} , 450 cm^{-1} and 475 cm^{-1}) where the differences lie outside of the measurement uncertainty estimates (Fig. 7(b)). Overall, for case A, a total of 1488 simulations were performed. Of these, 739 matched the observed spectrum to within uncertainties in the MIR and ~~a unique~~ 14 matched ~~(using method 4)~~ the observed spectrum in the FIR. ~~However, as implied by Fig. 7, the simulations that matched in the FIR were not contained within the set of simulations that matched in the MIR.~~ This result shows that for the bulk optical models tested, any combination of τ_{355} and

320 r_{eff} is unable to match the TAFTS and ARIES observations simultaneously within measurement error. Analysis of cases B and C (not shown) yields similar conclusions.

It is worth reiterating that the difference spectra obtained using method 3 demonstrate that it is possible to achieve excellent agreement in the MIR using MIR observations in isolation (Fig. 7(a)). However, extending the best fitting parameters to the FIR generates large residuals (Fig. 7(b)), while using the FIR in isolation yields closer agreement across the FIR (albeit not 325 within measurement uncertainty across all micro-windows) but even larger residuals in the MIR. This highlights that the combined use of MIR and FIR ~~information measurements should~~ provides a much tighter constraint on ~~the ability of any given ice cloud optical property model to capture the observed radiative behaviour of cirrus across the infrared spectrum, retrieval quality (consistent with Libois and Blanchet, [2017])~~ and that FIR observations are needed to refine and test bulk ice cloud optical model development.

330 To assess the energetic impact of misrepresenting the cirrus spectral signature, a first order estimate of the upwelling flux difference between the simulations selected by ~~all minimisation~~ methods (1-3-4) and the observations is obtained by multiplying the upwelling nadir radiances by π (assuming an approximation to the diffusivity-factor approximation, [Elsasser 1942]) and integrating over selected spectral ranges (Table 4). For completeness, results from all three cases analysed are shown. Table 4 indicates that, in all cases and for all methods there is a compensation effect between the differences seen in 335 the MIR and in the shortwave FIR channel. This compensation means that for Methods 1 and 2, rather large differences (of the order $0.6\text{--}1.6 \text{ W m}^{-2}$) are seen in the individual bands but these are somewhat masked when looking at the deviation integrated across all three bands. Our results suggest that the use of information solely from the MIR to estimate the cirrus properties (method 3) can result in sizeable deviations in both the SW FIR and the total flux, exceeding 2.0 W m^{-2} for one of the cases analysed. Using the FIR only (method 4), can lead to even greater deviations exceeding 3.0 W m^{-2} dominated by 340 differences in the MIR.

Discussion and Conclusions

The ability to simulate the radiative signatures of cirrus cloud across the mid- and far-infrared as measured by the ARIES and TAFTS instruments on the FAAM aircraft has been assessed using sophisticated radiative transfer codes in combination with state-of-the-art cirrus optical property databases. Despite considering a wide range of cloud properties, comparisons between 345 the simulated and observed spectra have shown that it is currently not possible to achieve agreement across the infrared to within the estimated measurement uncertainties for the Baum et al. [2014] bulk optical (~~single scattering~~) property models tested here.

With use of a variety of minimisation approaches, we have shown that restricting the matching frequency range to the mid-infrared generates multiple solutions that span a wide range of cirrus optical properties. These can give agreement with the 350 observations to within measurement uncertainty in the mid-infrared but result in discrepancies that exceed measurement uncertainty at far-infrared frequencies. While no solutions are able to simultaneously capture the observed mid and far-infrared

behaviour to within uncertainties, the combined use of the mid- and far-infrared gives the tightest constraint on optical model parameters thus enabling the identification of the most representative optical properties for the observed cloud.

First order analysis of the longwave energetic flux errors that result from deficiencies in the simulations' ability to represent the radiative properties of the observed thin cirrus demonstrate that these can be significant, reaching of the order of 1 to 2 Wm⁻² across the far-infrared for simulations that best match the mid-infrared in isolation. Deviations are even higher, reaching 3 Wm⁻² across the mid-infrared for simulations that best match the far-infrared measurements in isolation. Interestingly, these errors tend to compensate when summed across the infrared as a whole and would not be very apparent in broadband flux measurements. This illustrates the need for spectral information, since spectrally dependent errors would also be expected to translate into errors in the vertical profile of heating [e.g. Clough et al., 1995; Brindley and Harries, 1998; Turner et al., 2018] potentially affecting cloud and atmospheric dynamics.

It is noted that the ice cloud optical property databases employed in this study do not yet take into account the temperature dependency of the refractive indices of ice [Iwabuchi and Yang, 2011]. This is particularly important in the far-infrared as they show that the spectral effects of this temperature dependence on the ice optical properties has the greatest impact on the scattering between ~ 200 to 330 cm⁻¹ and on the absorption between 250 and 500 cm⁻¹, and that initial studies imply that this may can exert a noticeable impact on retrievals of cirrus optical depth and effective radius utilising the MIR-mid- and FIR-far-infrared simultaneously [P. Yang, pers. comm., 2019 Saito et al., 2020]. Other parameters included in the optical property databases, such as ice particle roughness, which although observed to be less important than habit and size [Maestri et al. 2019], may also require consideration in future. A further question relates to the relative sensitivity of the far- and mid-infrared regimes to depth within the cloud. To address this, the impact of varying the vertical profile of r_{eff} within the cloud on the simulated spectra was also considered (not shown), but was found to have an almost identical spectral signature to that generated by a bulk change in r_{eff} but of a greatly reduced magnitude, only a minor impact (typically <0.05 K).

Within the Baum et al. [2014] bulk optical models there is also an implicit assumption that the cloud PSD follows a gamma distribution. However, these PSDs were generated from in situ aircraft measurements from a variety of 11 field campaigns [Heymsfield et al., 2013]. How realistic these fitted PSDs may be for the clouds studied here is an open question; however using PSDs generated from the in situ measurements of the cloud microphysics for this campaign, obtained taken one hour over a period between 50 minutes to a little over two hours after the radiation measurements, does not improve upon the simulation performance. We note again that the high variability of the cloud field also raises questions as to how closely these in situ measurements represent the cloud sampled by the radiation instruments. Future campaigns should seek to employ a dual platform approach to enable simultaneous in-cloud sampling and above cloud radiative observations.

The European Space Agency recently announced the selection of its ninth Earth Explorer mission, Far-infrared Outgoing Radiation Understanding and Monitoring (FORUM), scheduled for launch in the 2025 timeframe. The mission will see the Earth's emitted radiation from 100 to 1600 cm⁻¹ measured from sun-synchronous orbit, providing global coverage for at least 4 years. These observations should enable a consistent link to be made between the microphysical properties of cirri and their

radiative signatures, ultimately helping to provide an improved representation of cirrus clouds in climate and forecast models, both in terms of the physical processes driving specific types of cirri formation and their associated impact on the Earth's energy budget. Key preparatory steps will be the development of bulk optical property models for ice cloud that show consistency with measurements across the electromagnetic spectrum, necessitating additional airborne observations of cirrus 390 and their associated microphysical properties over a range of cirrus types in addition to the optically thin frontal cloud analysed here.

Data availability

Data from the CIRCCREX field campaign can be found at the Natural Environment Research Council's Data Repository for Atmospheric Science and Earth Observation: <https://catalogue.ceda.ac.uk/uuid/6ba397d6c8854da19bcced8ea588c1f9>.

395 Author contributions

RB performed the simulations and designed and co-wrote the manuscript. HB provided guidance and focus for the study and co-wrote the manuscript. JM, AL and JP were responsible for enabling the measurements from the TAFTS instrument as part of the CIRCCREX campaign flight B895. CF provided some background material. SF and RH provided ARIES and LiDAR data. PY and BB provided ice cloud optical models and guidance. KB and SO provided information on the in situ microphysical 400 data obtain during the CIRCCREX campaign flight B895. JR and HO provided guidance and scientific feedback for the study.

Competing interests

The authors declare that they have no conflict of interest.

Acknowledgements

This study was funded by ESA contract number 4000124917. The CIRCCREX campaign and subsequent data analyses were 405 funded by the Natural Environment Research Council (UK) grants NE/K015133/1 and NE/K01515X/1.

References

Anderson G., Chetwynd, J., Clough, S., Shettle, E. and Kneizys, F.: AFGL atmospheric constituent profiles (0–120 km). Technical Report, U.S. Air Force Geophysics Laboratory, Hanscom Air Force Base, MA. p. 01731, 1986.

Bantges, R. J., Russell, J. E. and Haigh, J. D.: Cirrus cloud top-of-atmosphere radiance spectra in the thermal infrared. J. Quant. 410 Spect. Radiat. Trans., 63, 487-498, 1999.

Baran, A.: The dependence of cirrus infrared radiative properties on ice crystal geometry and shape of the size-distribution function, *Q. J. R. Meteorol. Soc.*, 131, 1129–1142, doi:10.1256/qj.04.91, 2005.

Baran, A.: The impact of cirrus microphysical and macrophysical properties on upwelling far-infrared spectra, *Q. J. R. Meteorol. Soc.*, 133, 1425–1437, doi:10.1002/qj.132, 2007.

415 Baran, A.: From the single-scattering properties of ice crystals to climate prediction: A way forward, *Atmos. Res.*, 112, 45–69, doi:10.1016/j.atmosres.2012.04.010, 2012.

Baran, A. and Francis, P.: On the radiative properties of cirrus cloud at solar and thermal wavelengths: A test of model consistency using high-resolution airborne radiance measurements, *Q. J. R. Meteorol. Soc.*, 130, 763–778, doi:10.1256/qj.03.151, 2004.

420 Baran, A., Cotton, R., Furtado, K., Havemann, S., Labonnote, L.-C., Marenco, F., Smith, A. and Thelen, J.-C.: A self-consistent scattering model for cirrus. II: The high and low frequencies, *Q. J. R. Meteorol. Soc.*, 140, 1039–1057, doi:10.1002/qj.2193, 2014a.

Baran, A., Hill, P., Furtado, K., Field, P. and Manners, J.: A coupled cloud physics-radiation parameterization of the bulk optical properties of cirrus and its impact on the Met Office Unified Model Global Atmosphere 5.0 configuration, *Journal of Climate*, 27, 7725–7752, 2014b.

425 [Baran, A. J., Furtado, K., Labonnote, L. –C., Havemann, S., Thelen, J. –C. and Marenco, F.: On the relationship between the scattering phase function of cirrus and the atmospheric state. *Atmos. Chem. Phys.*, 15, 1105–1127, doi:10.5194/acp-15-1105-2015, 2015.](#)

Baum, B., Heymsfield, A., Yang, P. and Bedka, S.: Bulk Scattering Properties for the Remote Sensing of Ice Clouds. Part I: 430 Microphysical Data and Models, *J. Appl. Meteorol.*, 44, 1885–1895, 2005a.

Baum, B., Yang, P., Heymsfield, A., Platnick, S., King, M., Hu, Y. and Bedka, S.: Bulk Scattering Properties for the Remote Sensing of Ice Clouds. Part II: Narrowband Models, *J. Appl. Meteorol.*, 44, 1896–1911, 2005b.

Baum, B., Yang, P., Nasiri, S., Heidinger, A. K., Heymsfield, A. and Li, J.: Bulk Scattering Properties for the Remote Sensing 435 of Ice Clouds. Part III: High-Resolution Spectral Models from 100 to 3250 cm^{–1}, *J. Appl. Meteorol. Climatol.*, 46, 423–434, doi:10.1175/JAM2473.1, 2007.

Baum, B., Yang, P., Heymsfield, A., Schmitt, C., Xie, Y., Bansemer, A., Hu, Y.-X. and Zhang, Z.: Improvements in Shortwave Bulk Scattering and Absorption Models for the Remote Sensing of Ice Clouds, *J. Appl. Meteorol. Climatol.*, 50, 1037–1056, doi:10.1175/2010JAMC2608.1, 2011.

Baum, B., Yang, P., Heymsfield, A., Bansemer, A., Cole, B., Merrelli, A., Schmitt, C. and Wang, C.: Ice cloud single-scattering 440 property models with the full phase matrix at wavelengths from 0.2 to 100 μm, *J. Quant. Spectrosc. Radiat. Transf.*, 146, 123–139, doi:10.1016/j.jqsrt.2014.02.029, 2014.

Bianchini, G. and Palchetti, L.: Technical Note : REFIR-PAD level 1 data analysis and performance characterization, *Atmos. Chem. Phys. Discuss.*, 8, 367–401, doi:10.5194/acpd-8-367-2008, 2008.

Brindley H. and Harries, J. E.: The impact of far IR absorption on clear sky greenhouse forcing, *J. Quant. Spec. Rad. Trans.*, 445 60, pp. 151-180, 1998.

Canas, T., Murray, J., Harries, J. and Haigh, J.: Tropospheric Airborne Fourier Transform Spectrometer (TAFTS). Satellite Remote Sensing of Clouds and the Atmosphere II, 3220, 91–102, 1997.

Clough, S. A. and Iacono, M. J.: Line-by-line calculation of atmospheric fluxes and cooling rates: 2. Application to carbon dioxide, ozone, methane, nitrous oxide and the halocarbons, *J. Geophys. Res. Atmos.*, 100, D8, 16519-16535, 450 doi:10.1029/95JD01386, 1995.

Clough, S., Shephard, M., Mlawer, E., Delamere, J., Iacono, M., Cady-Pereira, K., Boukabara, S. and Brown, P.: Atmospheric radiative transfer modeling: a summary of the AER codes, *J. Quant. Spectrosc. Radiat. Transf.*, 91, 233–244, doi:10.1016/j.jqsrt.2004.05.058, 2005.

Chen, W-N., Chiang, C-W. and Nee, J-B.: Lidar ratio and depolarization ratio for cirrus clouds, *Appl. Opt.*, 41, 6470-6476.
455 doi: 10.1364/AO.41.006470, 2002.

Cox, C., Harries, J., Taylor, J., Green, P., Baran, A., Pickering, J., Last, A. and Murray, J.: Measurement and simulation of mid- and far-infrared spectra in the presence of cirrus, *Q. J. R. Meteorol. Soc.*, 136, 718–739, doi:10.1002/qj.596, 2010.

Dee, D. P., and co-authors: The ERA-Interim reanalysis: configuration and performance of the data assimilation system. *Q. J. R. Meteorol. Soc.*, 137, 553-597, doi:10.1002/qj.828, 2011.

460 Dessler, A.E. and Yang, P.: The distribution of tropical thin cirrus clouds inferred from Terra MODIS data, *J. Climate*, 16, 1241-1247, doi:10.1175/1520-0442(2003)16<1241>LTDOTTC>2.0.CO;2, 2003.

Di Natale, G., Palchetti, L., Bianchini, G. and Del Guesta, M.: Simultaneous retrieval of water vapour, temperature and cirrus clouds properties from measurements of far infrared spectral radiance over the Antarctic Plateau, *Atmos. Meas. Tech.*, 10, 825-837, 2017.

465 Dlugokencky, E.J., Mund, J.W., Crotwell, A. M., Crotwell, M. J. and Thoning, K. W.: Atmospheric Carbon Dioxide Dry Air Mole Fractions from the NOAA GML Carbon Cycle Cooperative Global Air Sampling Network, 1968-2019, Version: 2019-07, <https://doi.org/10.15138/wkgj-f215>, 2019.

Edwards, J. M. and Slingo, A.: Studies with a flexible new radiation code. I: Choosing a configuration for a large-scale model. Quart. J. Roy. Meteor. Soc., 122, 689–719, doi:10.1002/qj.49712253107, 1996.

470 Elsasser, W. M.: Heat Transfer by Infrared Radiation in the Atmosphere. Vol. 6, Harvard Meteorological Studies, Harvard University Press, 107 pp., 1942.

Fox, S., Mendrok, J., Eriksson, P., Ekelund, R., O’Shea, S. J., Bower, K. N., Baran, A. J., Harlow, R. C. and Pickering, J. C.: Airborne validation of radiative transfer modelling of ice clouds at millimetre and sub-millimetre wavelengths, *Atmos. Meas. Tech.*, 12, 1599-1617, doi:10.5194/amt-12-1599-2019, 2019.

475 Gouveia, D. A., Barja, B., Barbosa, H. M. J., Seifert, P., Baars, H., Pauliquevis, T. Artaxo, P.: Optical and geometrical properties of cirrus clouds in Amazonia derived from 1 year of ground-based lidar measurements, *Atmos. Chem. Phys.*, 17, 3619–3636, doi:10.5194/acp-17-3619-2017, 2017.

Harries, J., Carli, B., Rizzi, R., Serio, C., Mlynczak, M., Palchetti, L., Maestri, T., Brindley, H. and Masiello, G.: The far-infrared Earth. *Rev. Geophys.*, 46, doi:10.1029/2007RG000233, 2008.

480 Heymsfield, A. J. and 10 co-authors: Testing IWC retrieval methods using radar and ancillary measurements with in situ data, *J. Appl. Meteorol. and Climatol.*, 47, doi: 10.1175/2007JAMC1606.1, 2008.

Heymsfield, A. J., Schmitt, C., and Bansemer, A.: Ice cloud particle size distributions and pressure dependent terminal velocities from in situ observations at temperatures from 0° to -86°C. *J. Atmos. Sci.*, 70, 4123-4154, doi: 10.1175/JAS-D-12-0124.1, 2013.

485 Hong, Y. and Liu, G.: The characteristics of ice cloud properties derived from CloudSat and CALIPSO measurements, *J. Climate*, 28, 3880-3901, doi: 10.1175/JCLI-D-14-00666.1, 2015.

[Hong, Y., Liu, G. and Li, J.F.: Assessing the radiative effects of global ice clouds based on CloudSat and CALIPSO measurements. *J. Clim.*, 29, 7651–7674, doi:10.1175/JCLI-D-15-0799.1, 2016.](#)

Iwabuchi, H. and Yang, P.: Temperature dependence of ice optical constants: Implications for simulating the single-scattering properties of cold ice clouds. *J. Quant. Spec. Radiat. Transf.*, 112, 2520-2525, doi:10.1016/j.jqsrt.2011.06.017, 2011.

490 Kuo, C.-P., Yang, P., Huang, X., Feldman, D., Flanner, M., Kuo, C. and Mlawer, E. J.: Impact of multiple scattering on longwave radiative transfer involving clouds. *Journal of Advances in Modeling Earth Systems*, 9. <https://doi.org/10.1002/2017MS001117>, 2017.

Lawson, R., O'Connor, D., Zmarzly, P., Weaver, K., Baker, B. and Mo, Q.: The 2D-S (Stereo) Probe : Design and Preliminary 495 Tests of a New Airborne, High-Speed, High-Resolution Particle Imaging Probe, *J. Atmos. Ocean. Technol.*, 23, 1462–1477, 2006.

Libois, Q. and Blanchet, J. -P.: Added value of far-infrared radiometry for remote sensing of ice clouds, *J. Geophys. Res. Atmos.*, 122, 6541-6564, doi:10.1002/2016JD026423, 2017.

Loeb, N. G., Yang, P., Rose, F. G., Hong, G., Sun-Mack, S., Minnis, P., Kato, S., Ham, S. -H., Smith, J., Hioki, S. and Tang, 500 G.: Impact of ice cloud microphysics on satellite cloud retrievals and broadband flux radiative transfer model calculations. *J. Clim.*, 31, 1851–1864, doi:10.1175/JCLI-D-17-0426.1, 2018.

Maestri, T.: Spectral infrared analysis of a cirrus cloud based on Airborne Research Interferometer Evaluation System (ARIES) measurements, *J. Geophys. Res.*, 110, D06111, doi:10.1029/2004JD005098, 2005.

Maestri, T. and Rizzi, R.: A study of infrared diabatic forcing of ice clouds in the tropical atmosphere, *J. Geophys. Res.*, 108, 505 4139, doi:10.1029/2002JD002146, 2003.

Maestri, T., Rizzi, R., Tosi, E., Veglio, P., Palchetti, L., Bianchini, G., Di Girolamo, P., Masiello, G., Serio, C. and Summa, D.: Analysis of cirrus cloud spectral signatures in the far infrared, *J. Quant. Spectrosc. Radiat. Transf.*, 141, 49–64, doi:10.1016/j.jqsrt.2014.02.030, 2014.

[Maestri, T., C. Arosio, R. Rizzi, L. Palchetti, G. Bianchini and M. Del Guasta: Antarctic ice cloud identification and properties using downwelling spectral radiance from 100 to 1,400 cm⁻¹, *J. Geophys. Res. Atmos.*, 124, 4761-4781, doi:10.1029/2018JD029205, 2019.](#)

Marenco, F.: Capabilities and operation of the FAAM EZlidar. Met Office OBR Tech. Note. NO. 79, 2010.

Marenco, F., Johnson, B., Turnbull, K., Newman, S., Haywood, J., Webster, H. and Ricketts, H.: Airborne lidar observations of the 2010 Eyjafjallajökull volcanic ash plume. *J. Geophys. Atmos.*, 116, doi:10.1029/2011JD016396, 2011.

515 Masuda, K., Takashima, T. and Takayama, Y.: Emissivity of pure and sea waters for the model sea surface in the infrared window regions, *Remote Sens. Environ.*, 24, 313-329, 1988.

Mlawer, E. J., Turner, D. D., Paine, S. N., Palchetti, L., Bianchini, G., Payne, V. H., Cady-Pereira, K. E., Pernak, R. L., Alvarado, M. J., Gombos, D., Delamere, J. S. and Mlynczak, M. G.: Analysis of water vapour absorption in the Far-infrared and submillimeter regions using surface radiometric measurements from extremely dry location. *J. Geophys. Res. Atmos.*, 520 124, 8134-8160, doi:10.1029/2018JD029508, 2019.

O’Shea, S.J., and 12 co-authors: Airborne observations of the microphysical structure of two contrasting cirrus clouds. *J. Geophys. Res. Atmos.*, 121, 13510-13536, doi:10.1002/2016JD025278, 2016.

Palchetti, L., Di Natale, G. and Bianchini, G.: Remote sensing of cirrus cloud microphysical properties using spectral measurements over the full range of their thermal emission: Cirrus cloud far IR signature, *J. Geophys. Res. Atmos.*, 121, 525 10,804–10,819, doi:10.1002/2016JD025162, 2016.

Platnick, S., and 12 co-authors: The MODIS cloud optical and microphysical products: Collection 6 updates and examples from Terra and Aqua. *IEEE Trans. Geosci. Remote Sens.*, 55, 502–525, doi:10.1109/TGRS.2016.2610522, 2017.

Rothman L.S. and 48 co-authors: The HITRAN 2012 molecular spectroscopic database, *J. Quant. Spectrosc. Radiat. Trans.*, 130, 4-50, 2013.

530 Saito, M., Yang, P., Huang, X., Brindley, H. E., Mlynczak, M. G. and Kahn, B. H.: Spaceborne mid- and far-infrared observations improving nighttime ice cloud property retrievals. *Geophys. Res. Lett.*, in press, 2020.

Stamnes, K., Tsay, S. –C., Laszlo, I.: DISORT, a General-Purpose Fortran Program for Discrete-Ordinate-Method Radiative Transfer in Scattering and Emitting Layered Media: Documentation of Methodology, DISORT Report v1.1 available at: <http://www.libradtran.org/lib/exe/fetch.php?media=disortreport1.1.pdf>, 2000.

535 Turner, D.D.: Arctic mixed-phase cloud properties from AERI-lidar observations: Algorithm and results from SHEBA, *J. Appl. Meteor.*, 44, 427-444, doi:10.1175/JAM2208.1, 2005.

Turner, D.D., Shupe, M. D. and Zwink, A. B.: Characteristic atmospheric radiative heating rate profiles in Arctic clouds as observed at Barrow, Alaska. *J. Appl. Meteor. Clim.*, 57, 953-968, doi:10.1175/JAMC-D-17-0252.1, 2018.

Vaisala: Advanced AVAPS System for Airborne Weather Research, 1999.

540 Vaisala: Vaisala Dropsonde RD94 Technical Datasheet, 2010.

van Diedenhoven, B., and Cairns, B.: A flexible parameterization for shortwave and longwave optical properties of ice crystals and derived bulk optical properties for climate models. *J. Atmos. Sci.*, 77(4), 1245-1260, doi:10.1175/JAS-D-19-0193.1, 2020.

Voigt, C. and 64 co-authors: ML-CIRRUS, The airborne experiment on natural cirrus and contrail cirrus with the high-altitude long-range research aircraft HALO, *Bull. Amer. Meteorol. Soc.*, D15, 271-288, doi:10.1175/BAMS-D-15-00213.1, 2017.

545 Wilson, S., Atkinson, N. and Smith, J.: The development of an airborne infrared interferometer for meteorological sounding studies. *J. Atmos. Oceanic Tech.*, 16, 1912–1927, doi:10.1175/15200426, 1999.

Yang, H., Dobbie, S., Herbert, R., Connolly, P., Gallagher, M., Ghosh, S., Al-Jumur, S. and Clayton, J.: The effect of observed vertical structure, habits, and size distributions on the solar radiative properties and cloud evolution of cirrus clouds, *Q. J. R. Meteorol. Soc.*, 138, 1221–1232, doi:10.1002/qj.973, 2012.

550 Yang, P.: Spectral signature of ice clouds in the far-infrared region: Single-scattering calculations and radiative sensitivity study, *J. Geophys. Res.*, 108, 4569, doi:10.1029/2002JD003291, 2003.

Yang, P., Kattawar, G., Hong, G., Minnis, P. and Hu, Y.-X.: Uncertainties Associated With the Surface Texture of Ice Particles in Satellite-Based Retrieval of Cirrus Clouds—Part I: Single-Scattering Properties of Ice Crystals With Surface Roughness, *IEEE Trans. Geosci. Remote Sens.*, 46, 1940–1947, doi:10.1109/TGRS.2008.916471, 2008.

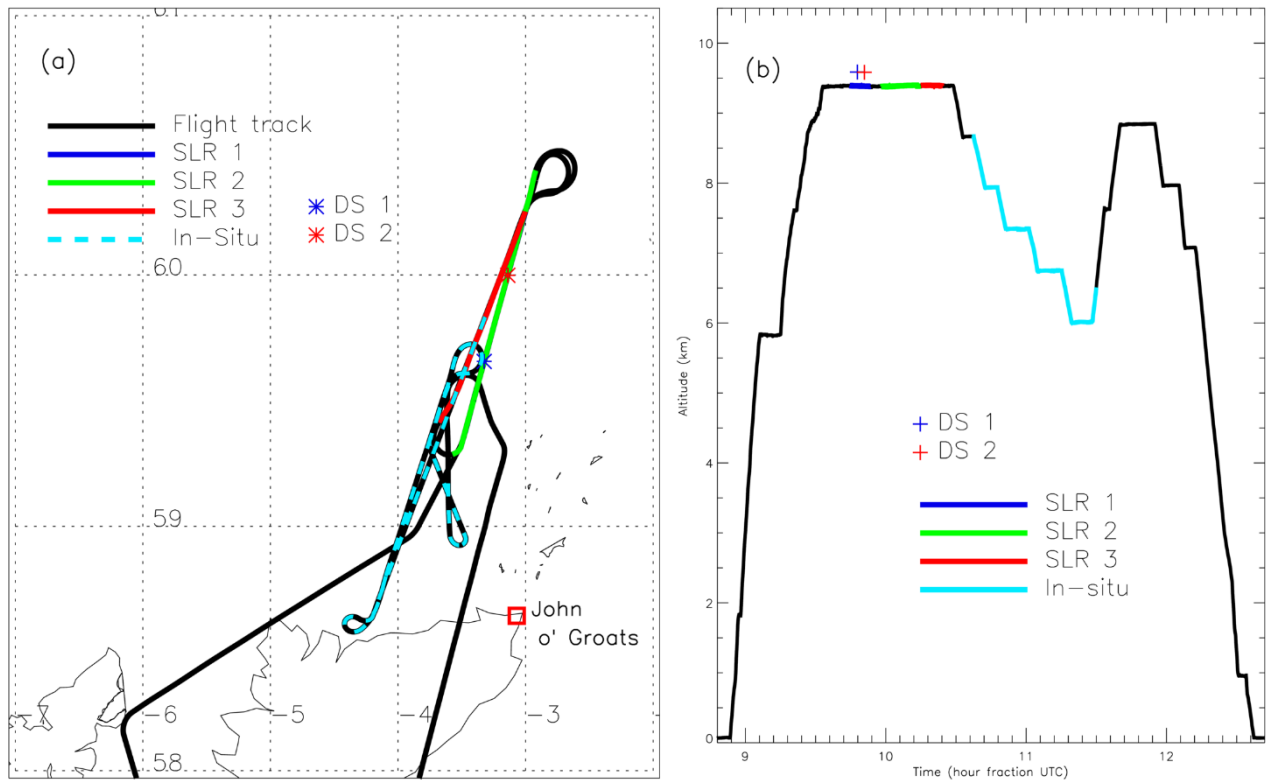
555 Yang, P., Bi, L., Baum, B. A., Liou, K-N., Kattawar, G. W., Mishchenko, M. I. and Cole, B.: Spectrally consistent scattering, absorption, and polarization properties of atmospheric ice crystals at wavelengths from 0.2 to 100 μm . *J. Atmos. Sci.*, 70, 330–347, 2013.

Yang, P., Liou, K.-N. , Bi, L., Liu, C., Yi, B. and Baum, B. A.: On the radiative properties of ice clouds: Light scattering, remote sensing and radiation parameterization. *Adv. in Atmos. Sci.*, 32(1), 32–63, doi:10.1007/s00376-014-0011-z, 2015.

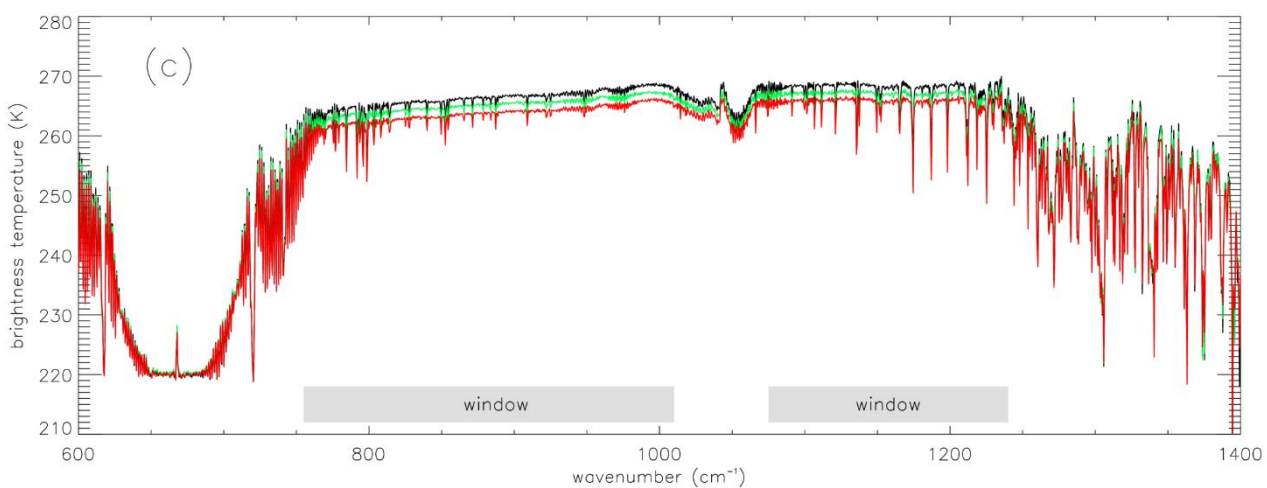
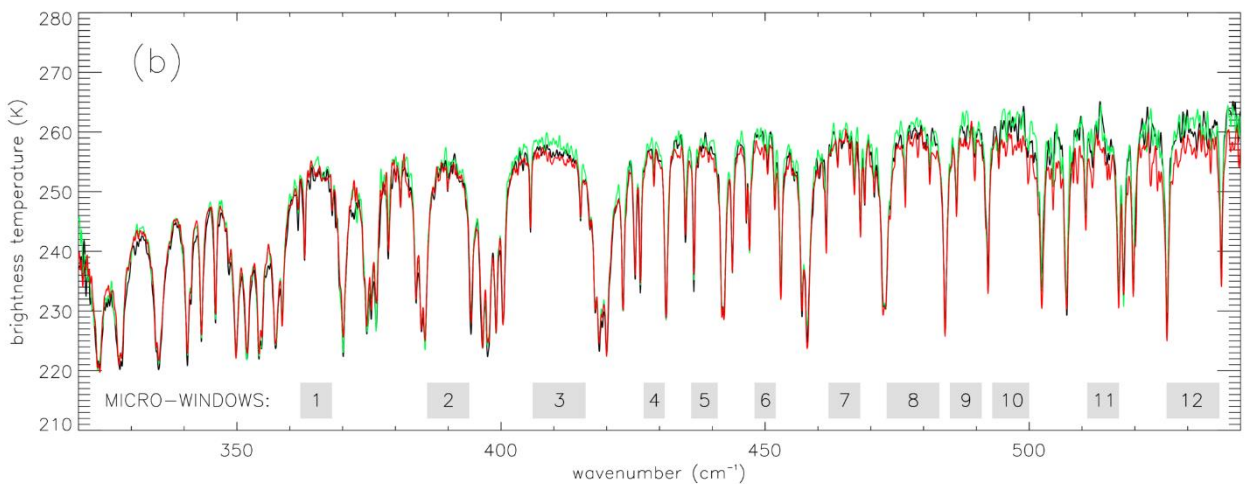
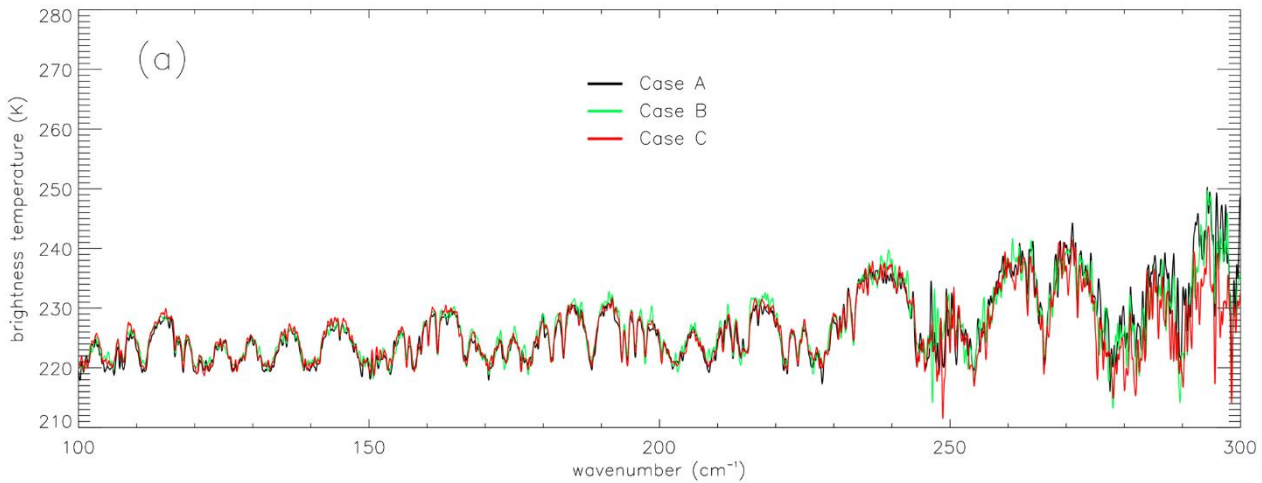
560 Yang, P., Hioki, S., Saito, M., Kuo, C.-P., Baum, B. A., & Liou, K.-N.: A review of ice cloud optical property models for passive satellite remote sensing, *Atmosphere*, 9, 499, doi:10.3390/atmos9120499, 2018.

Young, S. A., Vaughan, M. A., Kuehn, R. E., and Winker, D. M.: The Retrieval of Profiles of Particulate Extinction from Cloud-Aerosol Lidar and Infrared Pathfinder Satellite Observations (CALIPSO) Data: Uncertainty and Error Sensitivity Analyses, *J. Atmos. Ocean. Tech.*, 30, 395–428, doi:10.1175/JTECH-D-12-00046.1, 2013.

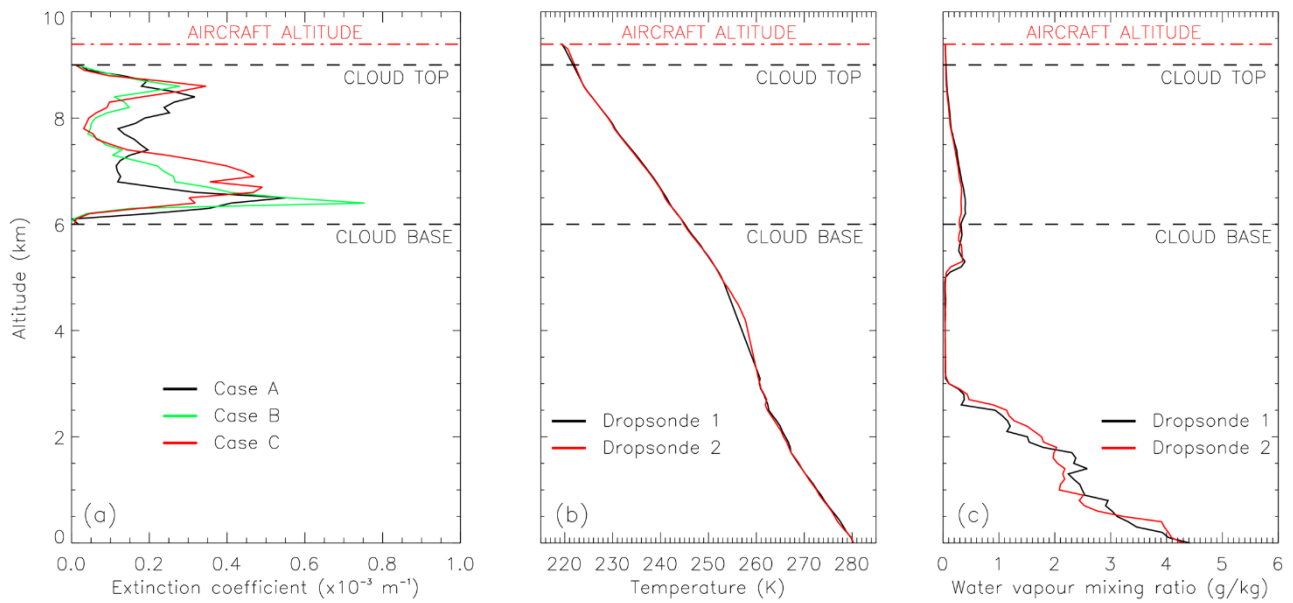
565 Zhang, Y., Macke, A. and Albers, F.: Effect of crystal size spectrum and crystal shape on stratiform cirrus radiative forcing, *Atmos. Res.*, 52, 59–75, doi:10.1016/S0169-8095(99)00026-5, 1999.



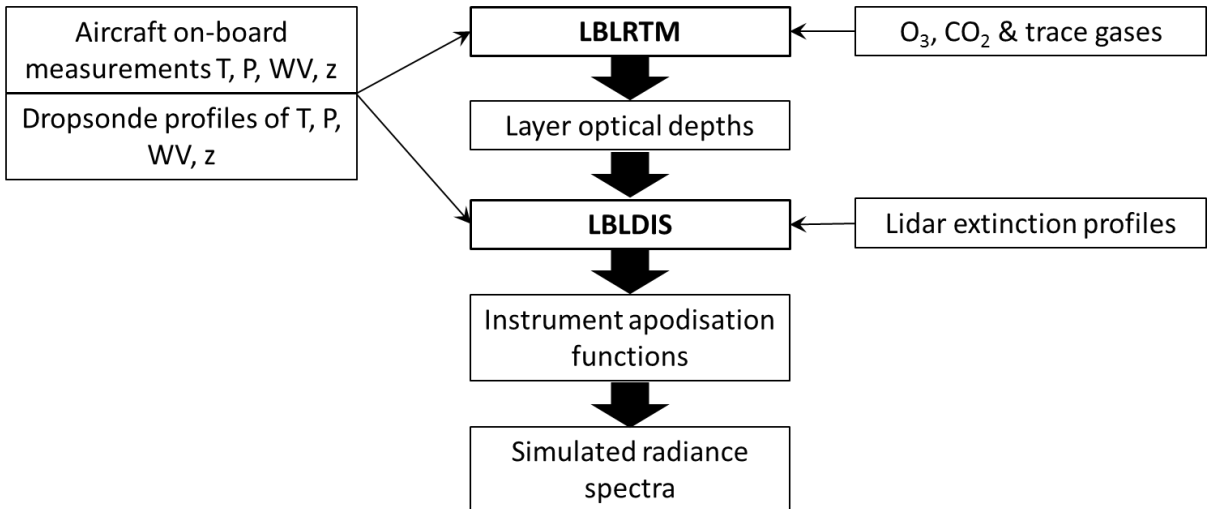
570 **Figure 1:** (a) Flight track for FAAM Flight B895 shown in black. The three SLRs are shown in colour, but note that SLR-1 lies directly beneath SLR-2 and is therefore not visible. The deployment of dropsondes (DS) 1 and 2 are indicated along with the period following SLR 3 when in situ sampling of the cloud layer was performed. (b) Aircraft altitude as a function of time, with the three SLRs and in situ measurement phases shown, and the DS 1 and 2 deployment times.



575 **Figure 2:** Brightness temperature spectra for the three cases A-C. (a): Individual TAFTS LW channel spectra. (b): Individual TAFTS SW channel spectra. (c): For each case, the mean of eight ARIES individual radiance spectra, converted to equivalent brightness temperature spectra. Also shown are a selection of atmospheric micro-window regions in (b), and the two main window regions in (c).



580 **Figure 3:** (a) Lidar extinction coefficient profiles for cases A to C. (b) Dropsonde temperature profiles from the two dropsondes deployed during SLR 1. (c) As (b) but for the water vapour mixing ratio profiles. The altitude of the aircraft and the upper and lower boundaries of the cirrus cloud layer are indicated by the black dashed lines.



585 **Figure 4:** Schematic of the inputs (T – temperature, P – pressure, WV – water vapour, z – altitude) and steps involved in simulating the radiance spectra observed by the TAFTS and ARIES spectrometers.

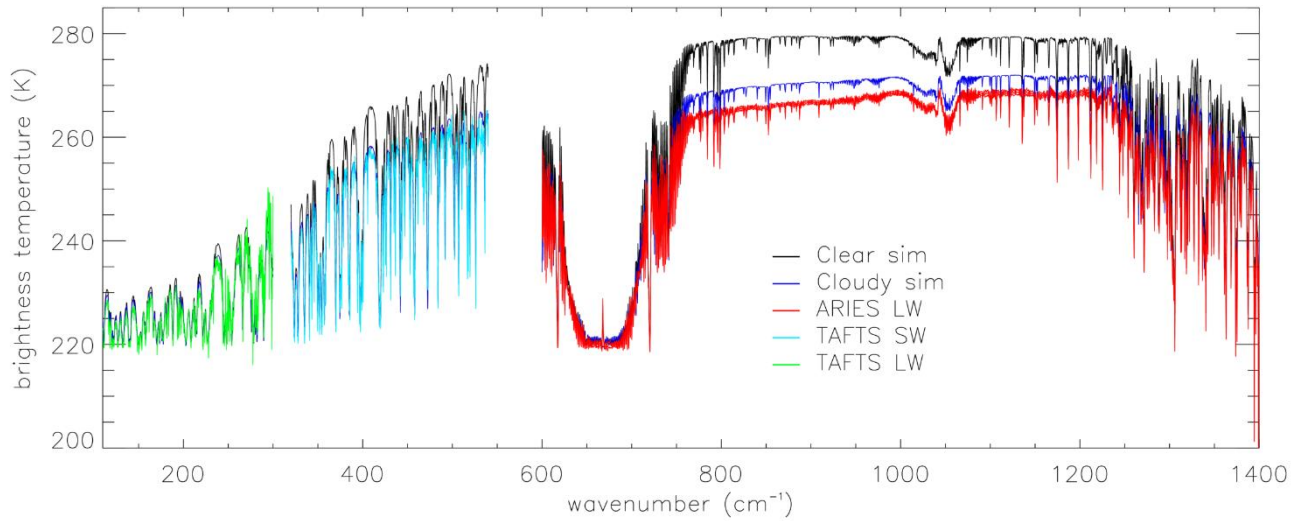
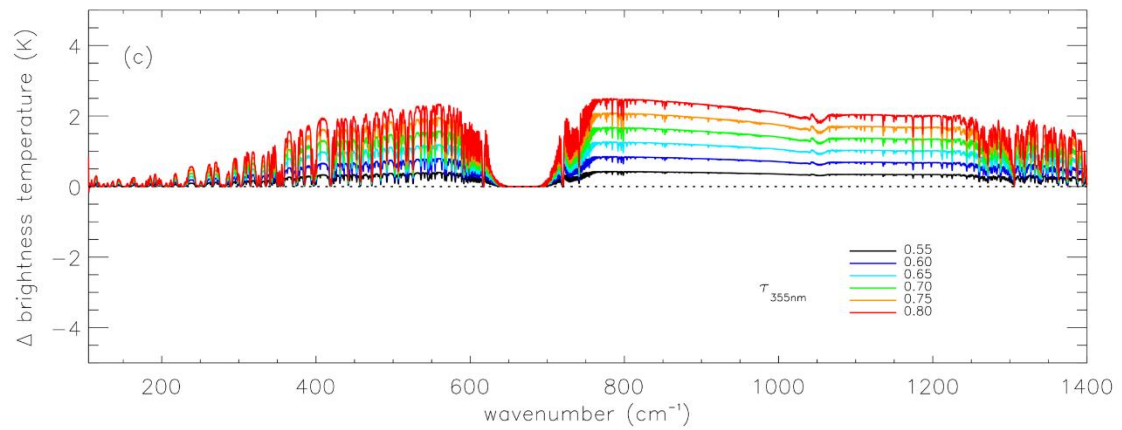
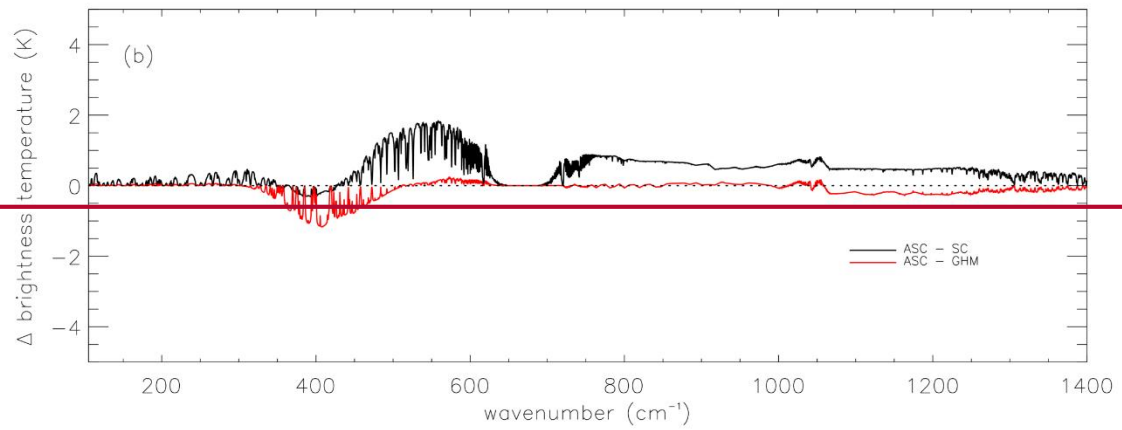
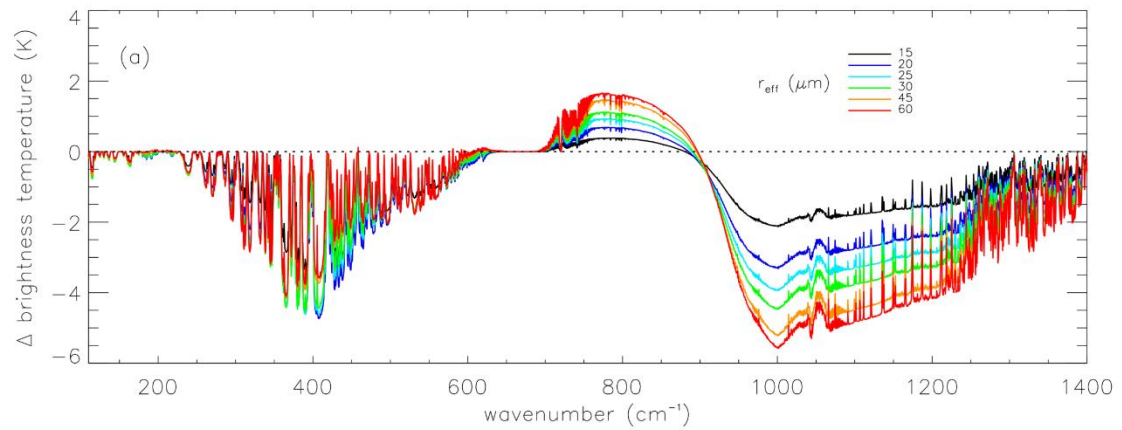
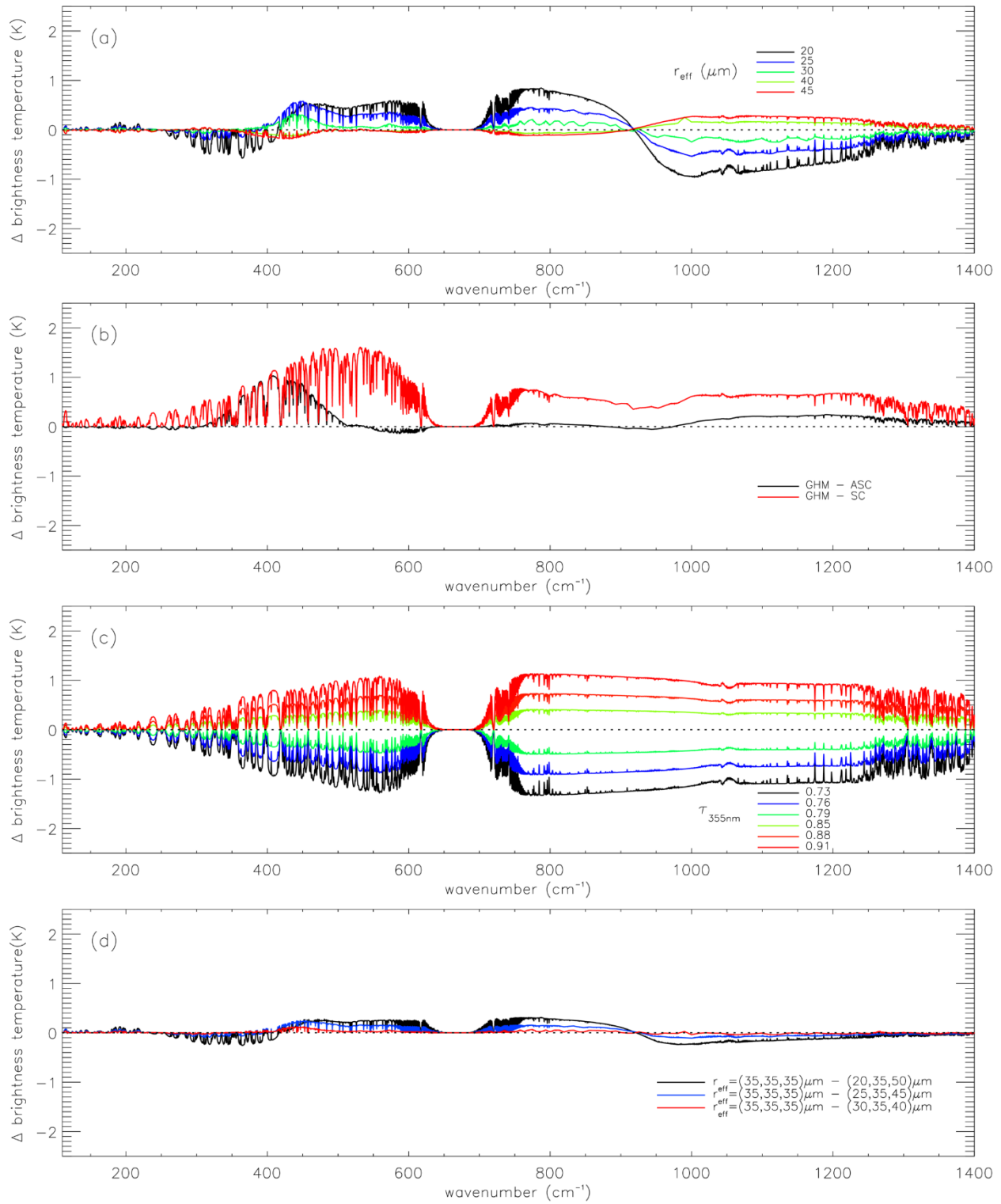
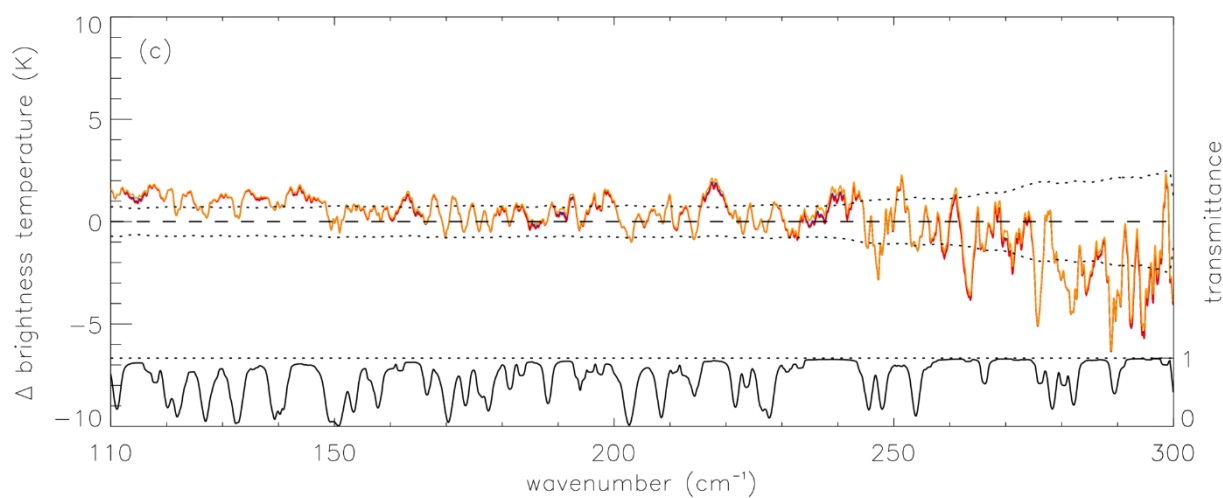
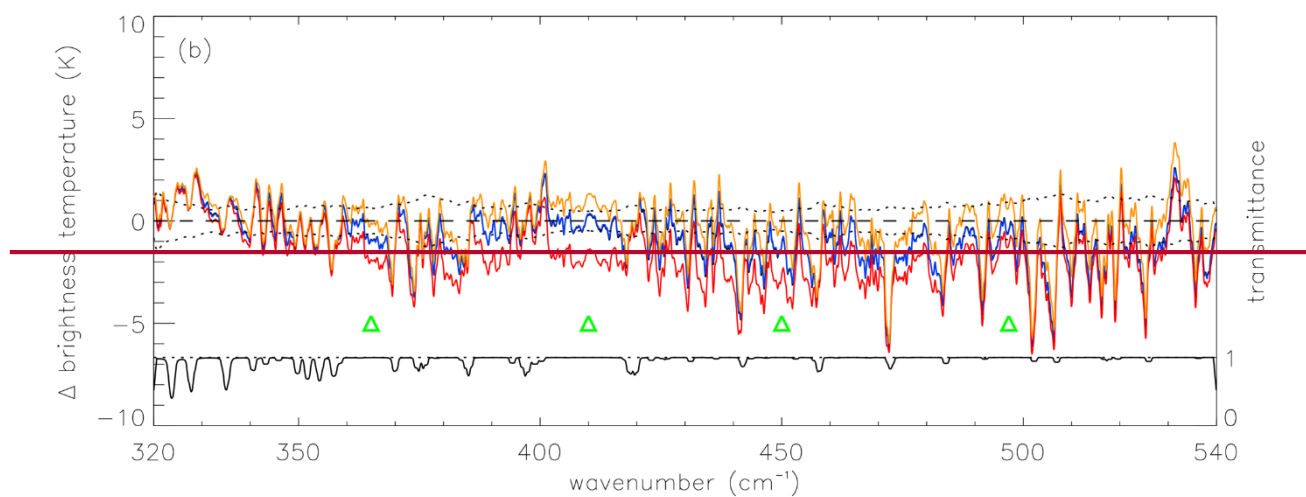
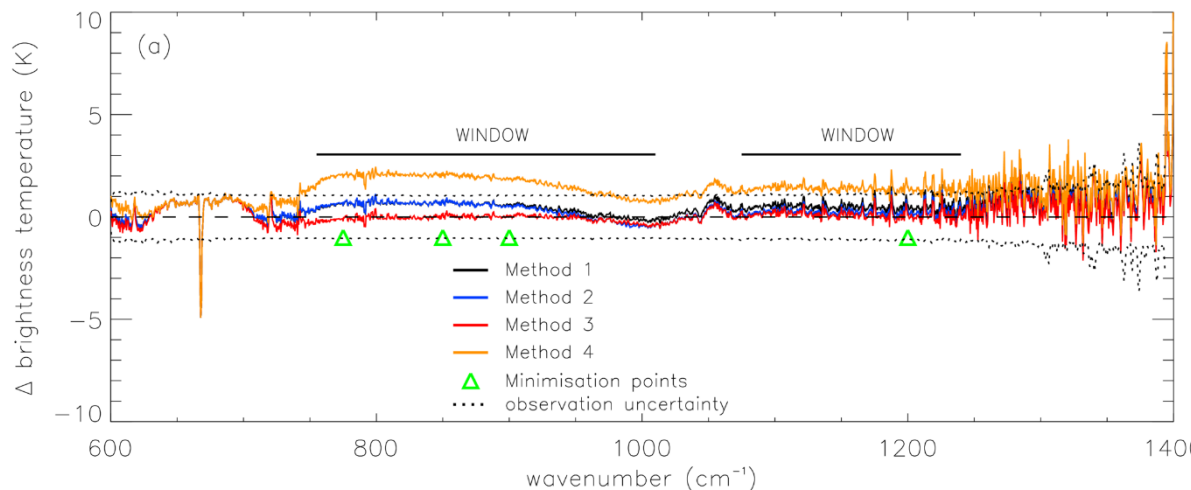


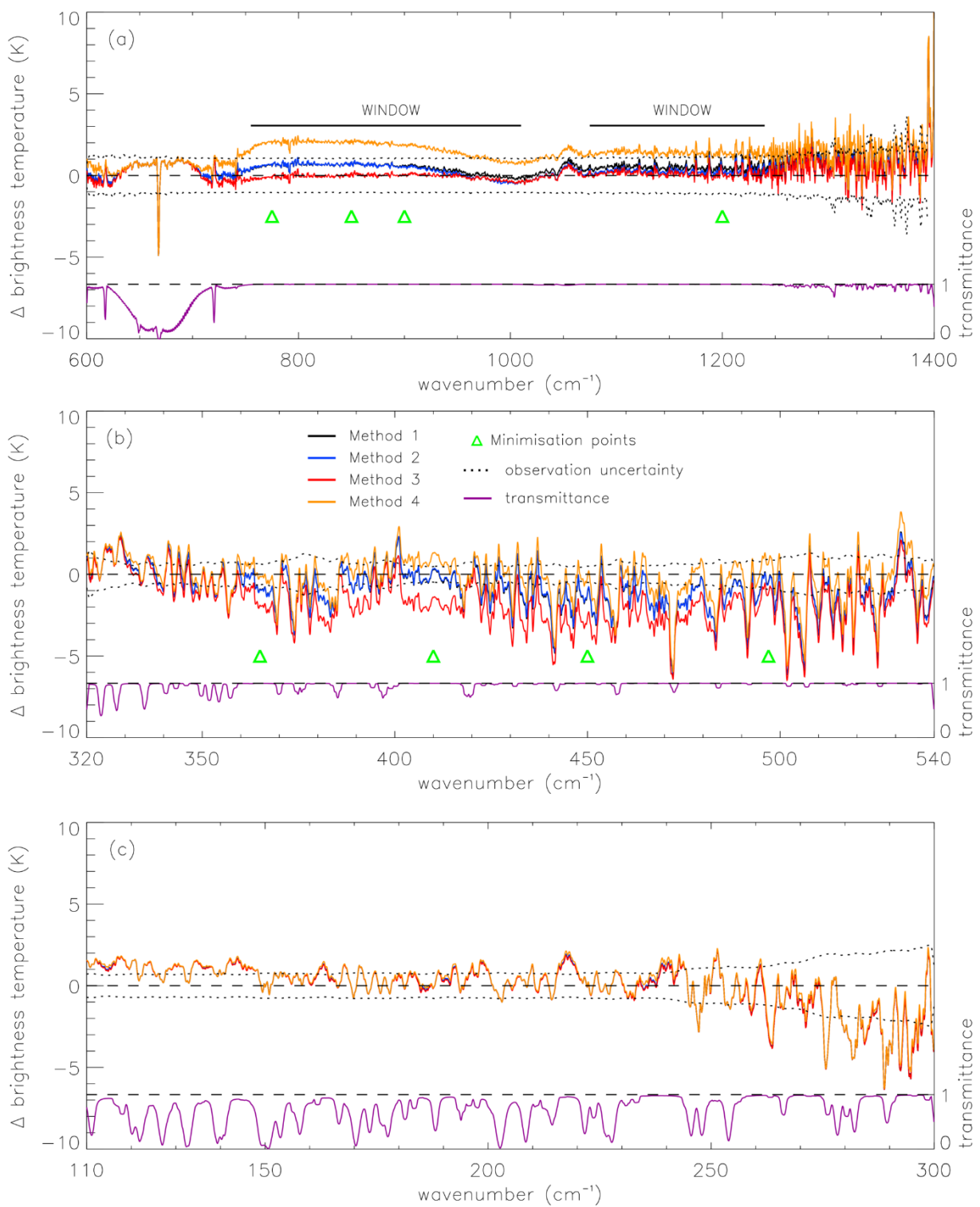
Figure 5: Simulation for case A assuming a cirrus cloud with $\tau_{355} = 0.584$, composed of ice particles with $r_{\text{eff}} = 30 \mu\text{m}$, and Baum ASC particle habit. The TAFTS LW and SW channel spectra are each a single spectrum. The ARIES LW channel spectrum plotted is a mean of 8 ARIES observations, and the width of the curve indicates the standard deviation about the mean.





595 **Figure 6: Simulated brightness temperature difference spectra to illustrate where there is sensitivity to r_{eff} (a), particle habit (b) and τ_{355} (c). Panel (d) illustrates the effect of varying r_{eff} in three 1 km thick layers through the cloud, with smaller crystals assumed at the top. In all panels, differences are relative to a simulation using the GHM model assuming $\tau_{355} = 0.82$ and $r_{\text{eff}} = 35 \mu\text{m}$. Panel (a) shows differences relative to a simulation using the ASC model assuming $\tau_{355} = 1.46$ and $r_{\text{eff}} = 10 \mu\text{m}$. Panel (b) shows differences relative to a simulation using the ASC model assuming $\tau_{355} = 0.87$ and $r_{\text{eff}} = 30 \mu\text{m}$. Panel (c) shows differences relative to a simulation using the ASC model assuming $\tau_{355} = 0.5$ and $r_{\text{eff}} = 30 \mu\text{m}$.**





600 **Figure 7: Simulation minus observation difference spectra for case A for each minimisation approach, for the (a) MIR, (b) SW FIR
and (c) LW FIR frequency ranges. The transmission of the atmosphere (derived from a simulation) between the cloud top and the
aircraft level is also shown ~~in the lower two panels~~.**

CASE	TAFTS obs. time (UTC) & sSM	ARIES obs. time (sSM)	LiDAR obs. time (sSM)	τ_{355}	Pressure at Aircraft (hPa)	Temperature at Aircraft (K)	Altitude at Aircraft (km)
A	09:48:39 35319	35318.3, 35318.8, 35319.3, 35319.8	35315	0.584	286.864	219.407	9.391
B	09:49:14 35354	35353.0, 35353.5, 35354.0 35354.5	35347	0.531	287.001	220.224	9.387
C	09:49:51 35391	35390.2, 35390.7, 35391.2 35391.7	35381	0.592	286.995	219.692	9.387

605 **Table 1:** Summary of the three cases (A,B and C) identified for use in this study, detailing the time of TAFTS, ARIES and LiDAR observations, along with the key variables from the on-board aircraft instrumentation obtained at the time of the TAFTS observations. Note that the TAFTS observation (obs.) times represent the UTC time (HH:MM:SS) and the equivalent seconds Since
610 Midnight (sSM) times. Also, note that there are 2 ARIES spectra (forward and reverse scan directions of the interferometer) associated with each ARIES observation time. The LiDAR time indicates the start of a 10 second period over which the data are averaged.

Case	Ice particle habit	τ_{355}	$r_{\text{eff}} (\mu\text{m})$
A	ASC, SC & GHM	0.5–73 to 0.918 at 0.012 resolution	20, 25 to 40 at 12 resolution, and 45
B	ASC, SC & GHM	0.87 to 1.03 at 0.01 resolution	20, 22, 25 to 40 at 1 resolution, and 45
C	ASC, SC & GHM	0.96 to 1.14 at 0.01 resolution	20, 22, 25 to 40 at 1 resolution, and 45

Table 2: Summary of the variation in the cloud **bulk** optical properties for which radiance spectra were simulated for cases A, B and C. For each case, the cloud optical depth vertical profile was scaled according to the corresponding lidar extinction profile. The effective radius of the ice particle size distribution were assumed constant for all layers within the cloud.

615

Method (approach)	Ice particle habit (A,B,C)	r_{eff} (A,B,C)	τ_{355} (A,B,C)
1	GHM, GHM, GHM	34, 38, 45	0.82, 0.93, 1.07
2	GHM, GHM, GHM	40, 38, 45	0.82, 0.93, 1.07
3	ASC, ASC, ASC	28, 31, 31	0.86, 0.97, 1.09
4	GHM, GHM, GHM	40, 45, 45	0.72, 0.86, 0.96

Table 3: Summary of the cloud optical properties that yield the closest agreement between the simulated and observed spectra for the four different minimisation approaches.

Approach number	600 to 1400 cm ⁻¹ (Wm ⁻²)			320 to 540 cm ⁻¹ (Wm ⁻²)			110 to 300 cm ⁻¹ (Wm ⁻²)			TOTAL (Wm ⁻²)		
	A	B	C	A	B	C	A	B	C	A	B	C
	1	1.10	0.92	0.69	-0.64	-1.55	-0.88	-0.08	-0.01	0.19	0.38	-0.64
2	0.84	0.92	0.69	-0.64	-1.55	-0.88	-0.08	-0.01	0.19	0.12	-0.64	0.00
3	0.17	0.22	0.31	-1.15	-2.02	-1.37	-0.09	-0.02	0.19	-1.07	-1.82	-0.87
4	3.30	2.51	3.03	-0.16	-1.20	-0.43	-0.06	0.00	0.21	3.08	1.31	2.81

Table 4: Integrated, simulation minus observation, flux differences for selected spectral ranges (MIR, SW FIR and LW FIR) and the total, for the best matching spectra obtained using the ~~first three~~^{four} different minimisation methods, for the three case studies. **Note, r**esults from method 4 are ~~not~~ included for completeness as although we do not anticipate future observations to be restricted to only FIR frequencies.